Global patterns of commodity-driven deforestation and associated carbon emissions

Chandrakant Singh[1,2] and U. Martin Persson[1]

[1]Department of Space, Earth and Environment, Chalmers University of Technology, Gothenburg, Sweden
[2]Stockholm Resilience Centre, Stockholm University, Stockholm, Sweden

Corresponding authors: Chandrakant Singh (chandrakant.singh@chalmers.se) and
U. Martin Persson (martin.persson@chalmers.se)

Abstract

Achieving global climate and biodiversity targets and ensuring future food security will require halting agriculture-driven deforestation. Accurate data on the commodities driving deforestation across time and space is crucial for informing policy development, implementation and evaluation. However, such information is currently hampered by limited and heterogeneous data availability (in both comprehensiveness and scope), computational challenges, and lack of updates to the existing databases, that diminish their accuracy and relevance over time. To tackle these challenges, we introduce the Deforestation Driver and Carbon Emission (DeDuCE) model, a framework that merges remotely sensed datasets with comprehensive agricultural statistics to enhance the quantification of agriculture and forestry-driven deforestation globally. Developed using Google Earth Engine and Python, DeDuCE is designed to integrate new and emerging datasets, ensuring the model remains efficient and relevant despite increasing data volumes. This approach also ensures adherence to FAIR data principles, emphasising replicability, adaptability and utility. DeDuCE reports over 9,100 unique country-commodity deforestation footprints across 176 countries and 184 commodities from 2001-2022, surpassing existing databases in scope and detail. The insights from DeDuCE are crucial for governments, companies, and financial institutions aiming to undertake deforestation and emissions accounting, risk assessments, and sustainability evaluations of investments.

Deforestation – the conversion of natural forests to make use of that land area for other activities – is a phenomenon of growing concern and far-reaching impacts[1]. The latest FAO's global forest resource assessment report suggests that over the past three decades, the world has lost forests equivalent to the size of India[2], with significant resulting impacts on climate change, biodiversity, and livelihoods[3,4]. When natural forests are cleared, they are often replaced by agricultural lands or forest plantations, which often lack the biodiversity and carbon storage capacity of the original forests. As a result, agriculture-driven deforestation is estimated to be the largest driver of biodiversity loss on land[5], constituting just under a tenth of total anthropogenic carbon emissions[6], and around a fifth of global food system greenhouse gas emissions[7]. The loss of these vital ecosystem services bears profound and enduring impacts on society, affecting the sustainability of our living environments and future food security.

At least 90% of global deforestation is driven by agriculture- and forestry-activities[1,8], a fact primarily explained by the escalating demands of a growing and increasingly affluent global population[9]. This increasing demand is not limited to products like cattle meat, vegetable oils, cocoa, coffee, and timber[10]; but also staple commodities such as rice, maize and cassava are being sourced from deforested lands[9]. Despite efforts to accurately quantify the impact of agricultural commodity production on deforestation and associated carbon emissions, uncertainties remain large, partly due to limitations in existing datasets[8]. While spatial datasets are available for some forest-risk commodities, they are often limited geographically and do not provide a comprehensive global view. Conversely, national and sub-national agricultural censuses offer comprehensive coverage of commodity production, but lack the spatial detail required for accurate deforestation attribution. Studies combining spatial and agricultural statistics are typically aggregated to national or sub-national scales[11]. Thus, efforts to link deforestation with agricultural and forestry-induced expansion at the pan-tropical or global scale are rare[8]. Among them, the majority rely primarily on statistical methods[12], and only a minority have utilised remotely sensed data to identify deforestation drivers[10,13]. This limited use of remotely sensed data at a global scale can be attributed to computational challenges in processing these datasets. Consequently, such studies often lack ongoing updates or refinements post-publication and tend to aggregate data over lengthy periods, limiting their accuracy and relevance over time.

An accurate understanding of deforestation dynamics – across time and space – is vital for shaping effective conservation policies and devising mitigation strategies for halting global forest loss. Policymakers, conservationists, and other relevant organisations – not the least corporate and finance actors – often lack reliable data to identify leverage points for interventions. A key example is the European Union's Deforestation Regulation (EUDR)[14]. Adopted in 2023, EUDR mandates companies to conduct due diligence in reporting deforestation-risk commodities (i.e., commodities that lead to deforestation) within their supply chains. This regulation necessitates the assessment of commodity-driven deforestation to combat deforestation and promote sustainable practices within European supply chains. With accurate data, stakeholders can make informed decisions that balance the need for food production with the imperative to preserve our remaining forest ecosystems and maintain a habitable climate. To assist with this, we introduce the Deforestation Driver and Carbon Emission (DeDuCE) model, a framework that melds the spatio-temporal precision of remote sensing and comprehensiveness of agricultural census data to track forest loss and link them with agriculture and forestry-induced deforestation globally.

1. Main text

1.1 State-of-the-art of the model

The DeDuCE model provides yearly estimates accounting the role of agriculture and forestry commodities in driving deforestation and associated carbon emissions. It delivers 9,106 unique deforestation carbon footprint estimations – encompassing 176 countries and 184 commodities (Supplementary Table 1 and 2) – between the period 2001 to 2022. It does so in the following way

(Fig. 1): The model overlays global spatio-temporal data of forest loss[15] with datasets on the extent of specific crops (e.g., soybeans[16], oil palm[17], cocoa[18], rubber[19]), land-uses (e.g., croplands[20], forest plantations[21] and pastures[22]), dominant deforestation drivers[23], and state of forest management[24]. Using a procedure that prioritises data with higher resolution – spatially, temporally, or in terms of deforestation driver specificity – the model identifies where deforestation is occurring (excluding forest losses in existing plantations or managed forests) and attributes this either directly to a specific commodity (e.g., soybeans), a specific land-use (e.g., cropland) or a mix of land-uses (e.g., mosaic of cropland and pastures) (Fig. 1). In the latter cases, where deforestation is spatially attributed to broad land-uses, the model uses agricultural and forestry census data (primarily at the national level[2,25]), to identify the commodities most likely to drive forest loss in a two-step statistical land-balance approach[12]: first, deforestation is attributed either to cropland, pastures or forest plantations based on their relative expansion; second, cropland deforestation is further attributed to different crop commodities based on their relative expansion in harvested area, while pasture deforestation is attributed to cattle meat and leather products and deforestation due to forest plantations to forestry products. Finally, we estimate the carbon losses due deforestation – accounting for carbon stored in above- and below-ground biomass, dead wood, litter and soils – by overlaying the spatial identification of deforestation drivers with data on forest[26] and soil[27] carbon stocks (Fig. 1). Net carbon emissions are then calculated by accounting for the carbon sequestered in the replacing land use. Furthermore, peatland emissions are determined by overlaying the identified deforestation drivers with the global extent of peatlands, followed by applying emission factors that are contingent on different land use and forest biomes.

We have done an extensive literature review to incorporate the latest datasets pertaining to land use and land-use change (LULUC), capturing the extent of deforestation across various commodities and land uses. As a result, the DeDuCE model provides deforestation footprints of agricultural and forestry commodities with an accuracy that greatly exceeds those in existing life cycle inventory (LCI) databases (e.g., Ecoinvent[28]), which are solely based on agricultural statistics (sometimes of limited quality) and default carbon emission factors, and thus do not account for the wealth of available remote sensing data. Further, the DeDuCE model includes emissions from peatland drainage on deforested land, a substantial contributor to agricultural land-use emissions.[29] Finally, the model aims to account for key land-use change dynamics – such as land competition between cropland, pasture and other land-uses, as well as cropland and pasture degradation and abandonment – important for the causal attribution of deforestation to agricultural commodity production, but poorly captured in existing LCI databases. In doing so, the model aims to identify the direct (or proximate) drivers of deforestation (i.e., the commodities that are produced on the deforested land), what in corporate greenhouse gas accounting guidances[30,31] is referred to as direct land-use change (dLUC). However, where commodity-specific spatial data is unavailable, the results from the statistical modelling reflect what these frameworks call statistical land-use change (sLUC), and should be interpreted as a measure of deforestation risk.

The DeDuCE model's versatility allows for the inclusion of diverse datasets, varying in spatial-temporal resolution and format (such as pixel and vector datasets). It is designed to be distinctively forward-looking, having the capacity to integrate emerging datasets, ensuring its relevance and adaptability in the future. The model's flexibility also allows for adjusting parameters, such as tree cover density for forest classification, lag periods between forest clearing and establishment of agricultural land systems, the handling of specific land uses and mixed-use mosaics; and control over attribution and amortisation period. Moreover, through quality assessment, we further strengthen the reliability of our deforestation attribution estimates, ensuring a comprehensive and nuanced understanding of agricultural-driven deforestation trends, and highlighting regions and commodities where further improvements are necessary to improve model estimates. Taken together, this enhances the model's utility as a tool for not only understanding, but supporting global sustainability and conservation efforts.

The DeDuCE model leverages the computational capabilities of Google Earth Engine (GEE), enabling the processing of terabytes of high-resolution spatial data, a task that is challenging on personal computers using conventional geographic information system (GIS) software. The utilisation of GEE's vast processing capabilities, combined with Python's open-source programming for statistical calculations, aligns with FAIR data policies, promoting accessibility and transparency. By adopting these technologies and principles, we aim not only to ensure data integrity and replicability, but also to foster community engagement, inviting researchers and stakeholders to contribute, enhance, and broaden the model's scope, ultimately making it a valuable resource for the broader community.

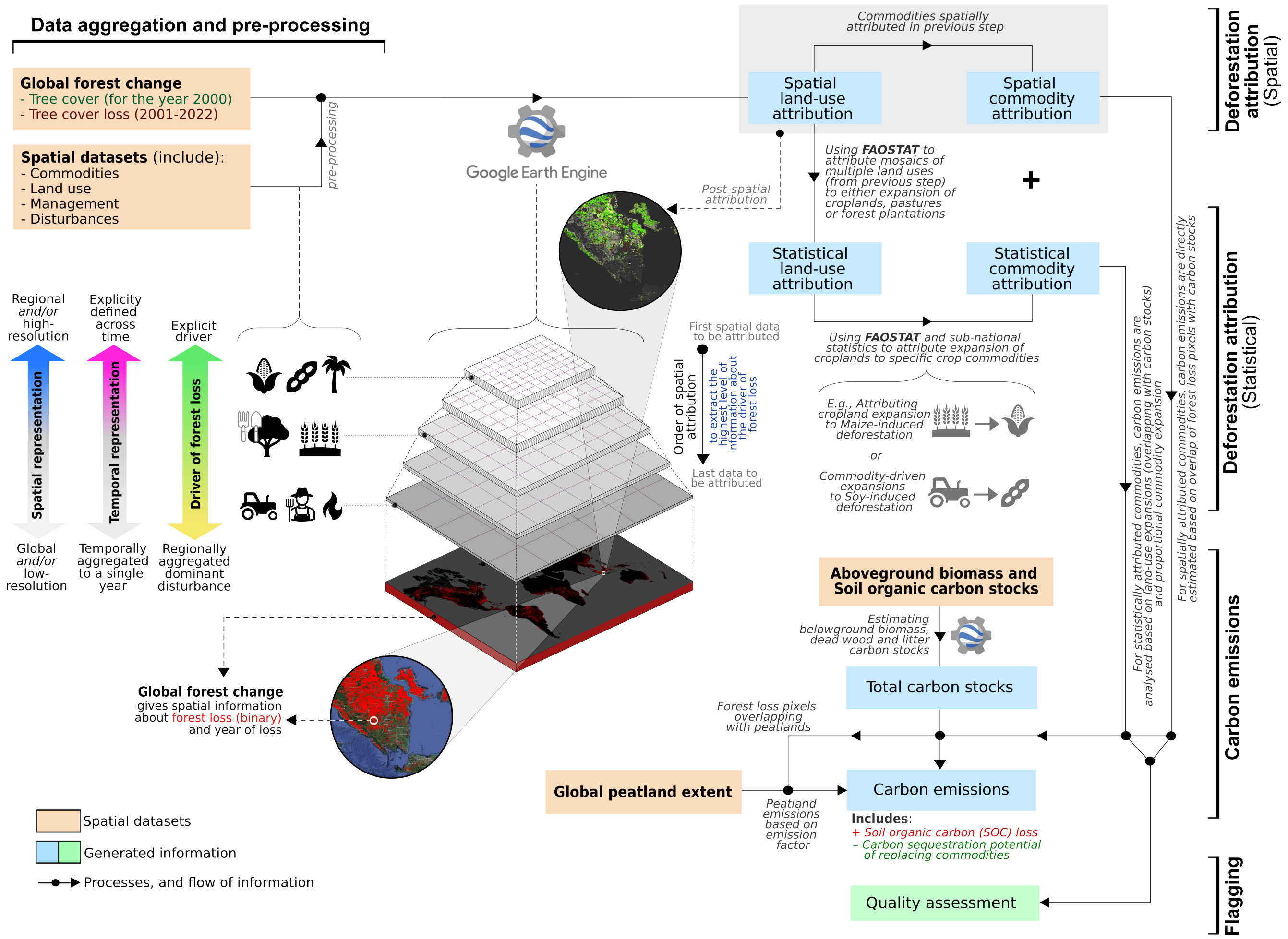

Fig. 1 | Framework for the Deforestation Driver and Carbon Emission (DeDuCE) model. This framework consists of three key components: deforestation attribution (spatial and statistical), carbon emission calculation, and flagging. In the first step, we utilise remote sensing and (sub-)national agricultural statistics to determine what portion of the total annual tree cover loss is attributable to specific commodities. From this, we next calculate carbon emissions linked to commodity-driven deforestation, incorporating emissions (including emissions from peatland drainage on deforested lands). Finally, we evaluate the reliability of our deforestation estimates by assessing the quality of the input data used in our analysis. A detailed description on the datasets used in this model is provided in Supplementary Table 3.

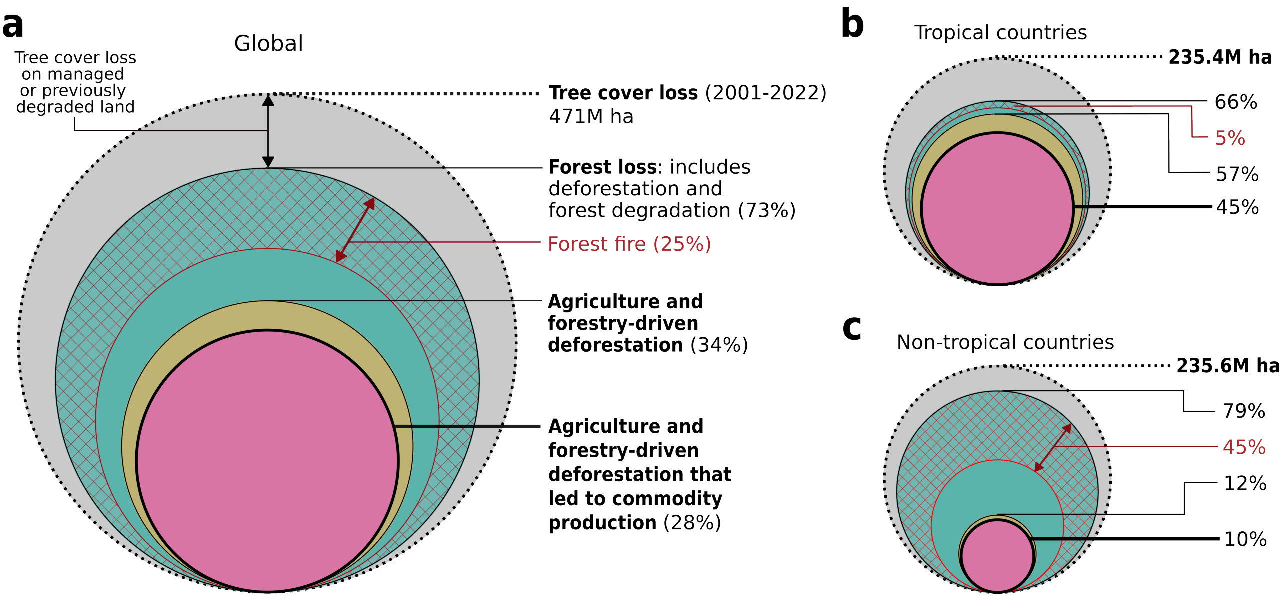

Fig. 2 | Assessing deforestation from global tree cover loss estimates. (a) The nested circles provide an insight into agriculture and forestry-driven deforestation derived from global tree cover loss estimates (refers to loss of tree canopy within a 30-m pixel globally between 2001-2022[15]; tree cover density ≥ 25%). Forest loss, which includes deforestation and forest degradation, captures the loss of natural forests by excluding loss on managed or degraded lands established before the year 2000 (e.g., rotational clearing on forest plantations or loss of sparse growth on degraded land systems). Within this, losses due to forest fires are indicated with hatch patterns. Additionally, the scope of agriculture and forestry-driven deforestation extends to include the instances where deforestation is directly linked to the production of commodities, and where it occurs independently of such production. The latter scenario is examined by evaluating the extent of agriculture and forestry-driven deforestation in land-use attribution (in Fig. 1) that cannot be linked to any specific commodity in commodity attribution in DeDuCE's land balance approach. Possible mechanisms where deforestation does not lead to the production of commodities are explored in ref.[8]. The size of the circles in the diagram is proportional to their respective shares in the total area of tree cover loss. To offer a comparative insight into deforestation dynamics across different biomes, in this figure, we have also separated our analysis for (b) tropical and (c) non-tropical countries. The design of the figure is inspired by ref.[8].

1.2 Key insights from application of the model

The results from DeDuCE reveal that of the 471 million hectares (Mha) of global tree cover loss observed from 2001 to 2022, only 28% is driven by expanding croplands, pastures, and forest plantations for commodity production (Fig. 2a). However, the share of these productive commodity-driven deforestation exhibits stark contrasts between tropical and non-tropical regions: 45% of the tree cover loss in tropical countries is attributed to expanding agricultural land and forest plantations, compared to just 10% in non-tropical counties (Fig. 2b,c). Compared to prior assessments of tropical forest loss[8], DeDuCE presents a lower overall estimate of agriculture and forestry-driven deforestation, yet it shows marginally higher figures for deforestation leading to production (Fig. 2b). This suggests that DeDuCE's incorporation of spatial datasets more accurately reflects deforestation resulting from land-use expansion in natural forests and rotational clearing in managed forests.

Interestingly, our analysis indicates that 6% of global forest loss that is attributed to agriculture and forestry-driven deforestation did not result in any identifiable production (Fig. 2a), with the figures standing at 12% for tropical and 2% for non-tropical countries (Fig. 2b,c). These relatively large discrepancies in tropical countries are often linked to challenges in land tenure clarity and disputes[8]. For instance, anticipation of future agricultural returns, planned infrastructural developments, uncertain future forest conservation legislations and availability of large expanses of undesignated public lands, often lead to speculative clearing[32,33] that can fail to evolve into productive agricultural or forestry ventures.

Our analysis also suggests an uneven distribution of both deforestation and the resulting carbon emissions across regions and commodities (Fig. 3): South America leads both in deforestation and carbon emission, with Southeast Asia and Africa also showing major contributions. Additionally, Southeast Aisa is also responsible for nearly 85% of global peatland drainage emissions. Together, these three regions account for roughly 84% of global deforestation due to expanding agriculture and forest plantations, and 93% of the carbon emissions linked to these activities. Still, two countries outside the tropics – China and the United States – closely trail the top three countries globally – Brazil, Indonesia, and the Democratic Republic of Congo (DR Congo) – in terms of deforestation area (though not in carbon emissions; Fig. 3a). In terms of specific commodity groups, deforestation primarily driven by pasture expansion represents about 40% of total deforestation and 46% of the carbon emissions (Figure 3b). The cultivation of oilseeds and oleaginous fruits, especially oil palm and soybeans, accounts for 17% of deforestation and 11% of carbon emissions. Other major contributors to deforestation include forest plantations, contributing to 14% of deforestation and 2% of carbon emissions, and cereals, responsible for 10% of deforestation and 12% of carbon emissions.

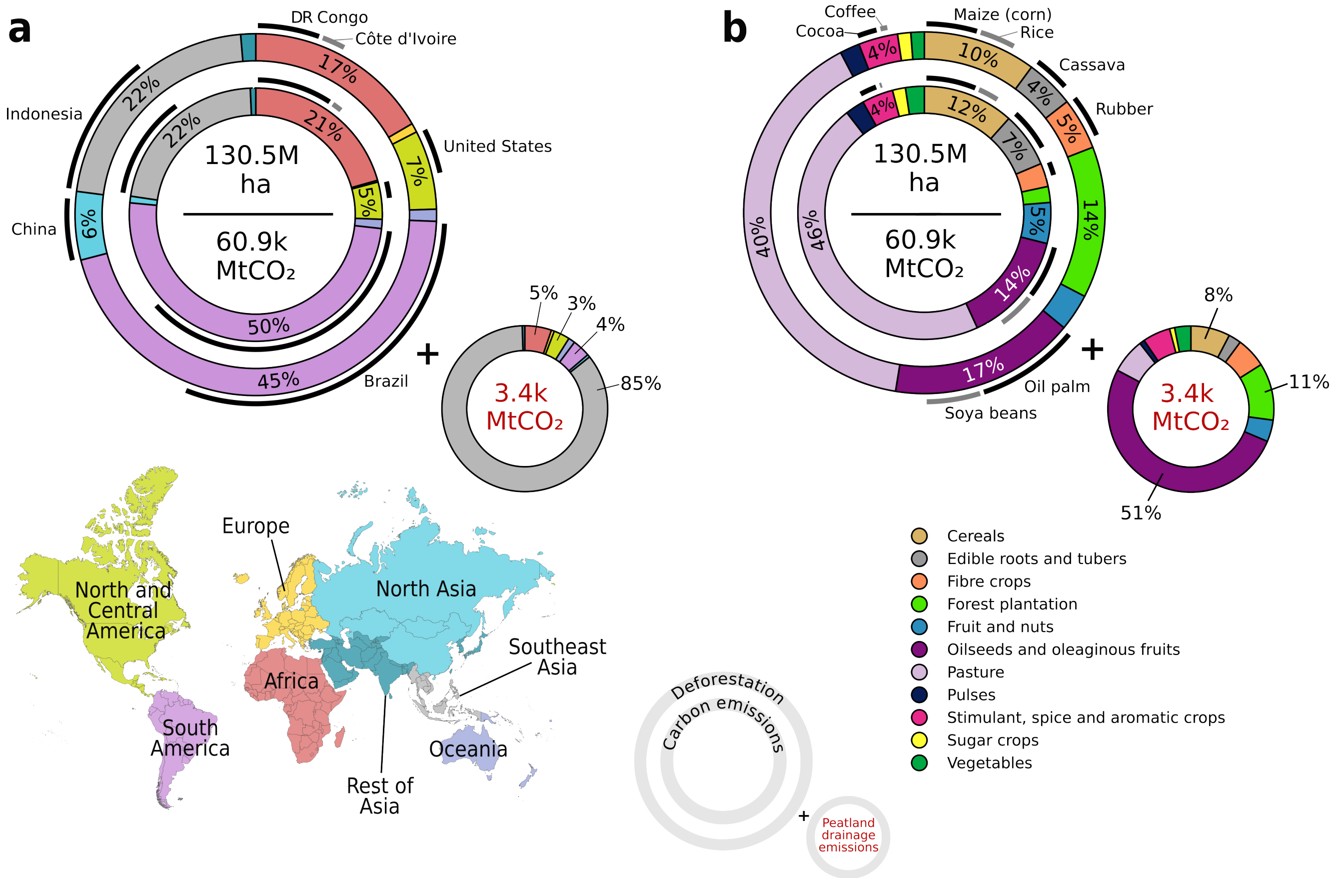

Fig. 3 | Global overview of deforestation and carbon emissions (2001-2022). This figure displays agriculture and forestry-driven deforestation and corresponding carbon emissions globally, categorised by (a) geographical regions and (b) commodity groups. In the concentric rings, the outer ring depicts the proportional deforestation by area, while the inner ring shows carbon emissions. Emissions from peatland drainage are presented separately. Central insets mention total deforestation (in ha) and carbon emissions (in $MtCO_2$), with selected major deforestation contributors and commodities accentuated along the periphery of the concentric circles.

Investigating the link between specific country-commodity pairs and deforestation (Supplementary Fig. 1-3), we find that in South America, the expansion of pastures for cattle meat production primarily influences the region's deforestation. However, in Paraguay, pasture expansions are linked to the growing demand for leather in the automotive industry[34], resulting in a surge in cattle ranching areas (Fig. 4 and Supplementary Fig. 3). Additionally, the cultivation of soya beans – closely linked to the livestock sector as feed for cattle and indirectly related dairy and egg production[35] – also leads to notable deforestation across the continent, and is considered to be an important indirect driver of deforestation through expansion into pastures[16,35], particularly in Brazil, Paraguay, Bolivia and Argentina[36].

In recent years, Brazil has witnessed a resurgence in deforestation rates (Fig. 4), driven by the relaxation of environmental regulations by local governments, particularly those allowing expansion into protected and indigenous territories, and the weakening of deforestation prevention law enforcement[37]. Similarly, Bolivia has seen increasing agriculture-driven deforestation in recent years by offering public lands at reduced prices to settlers (or smallholder farmers), lowering taxes on agricultural products and equipment, and granting amnesty for illegal deforestation[38,39] (Fig. 4 and Supplementary Fig. 3). These policies have motivated increased deforestation, illegal logging, the avoidance of restoring illegally deforested lands and encouraged land grabbing, thus accelerating the establishment of large-scale commercial agriculture and therefore deforestation in the region[37].

Oil palm and rubber plantations in Southeast Asia, particularly in Indonesia, Malaysia and Thailand, represent a major chunk of global deforestation (Fig. 3, Supplementary Fig. 2 and 3). The cultivation of oil palm stands out for its lucrative profit margins due to high yields, a surging global demand for vegetable oils[10], coupled with regional governments' efforts to boost production, significantly accelerating deforestation[17]. Furthermore, these plantations are frequently established on drained peatlands (Fig. 3b), leading to additional carbon emissions. Conversely, the deforestation linked to rubber cultivation is fuelled by its extensive use in the tyre industry, among other diverse industrial applications[19]. Interestingly, the deforestation rates for these commodities have shown sensitivity to global market trends, with noticeable declines during the early 2010s following a crash in the prices of oil palm and rubber[17,19] (Fig. 4). Moreover, there are instances where landholders show a preference for rubber over oil palm plantations in areas designated for oil palm concessions[40], particularly due to market liberalisation and the attractive prices and potentially increasing demand for rubber[41]. This may explain why deforestation rates linked to rubber cultivation do not exhibit the same level of volatility as those associated with oil palm (Fig. 4).

Cocoa and coffee, key cash crops integrated into the global diet, have contributed to rising deforestation rates, particularly in tropical nations like Côte d'Ivoire, Ghana, Indonesia, and Brazil (Fig. 3b, Supplementary Fig. 2 and 3). Despite their traditional cultivation being symbiotic with forest ecosystems[18,42], the surge in worldwide demand for these commodities has led to more intensive farming practices, driving deforestation[43] (Fig. 4). In addition to tropical cash crops, forest plantations play a substantial role in global deforestation (Fig. 3b). Most notably, in the United States and China, deforestation patterns due to forest plantations are on par with major commodity-country pairs (Supplementary Fig. 2 and 3), directly tied to the surging demand for timber and pulp driven by construction booms in these countries[44].

Our analysis also reveals that staple crops – specifically maize, cassava and rice – are significant drivers of deforestation (Fig. 3b, 4, Supplementary Fig. 2 and 3), exceeding cocoa and coffee in terms of both deforestation area and emissions. Despite their substantial role in global deforestation, these staple commodities often receive less attention, exemplified by their omission from the European Union Deforestation Regulation (EUDR)[14]. However, tracking deforestation linked to these staples is crucial, as their cultivation is expected to grow, propelled by the need to satisfy the dietary requirements of a burgeoning global population and the ensuing market demands[45].

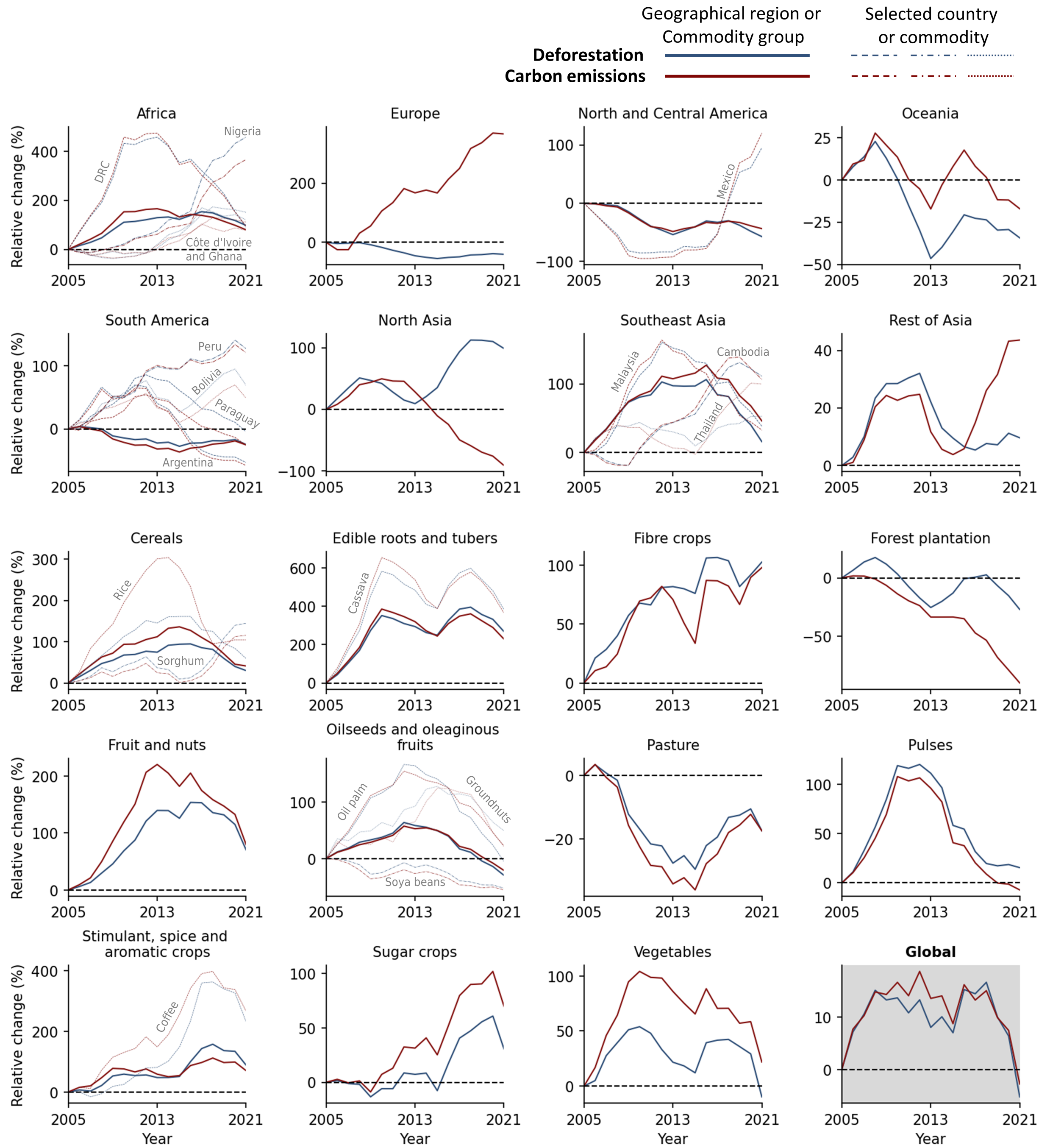

Fig. 4 | Temporal trends of deforestation and carbon emissions. This plot illustrates the relative changes in deforestation and carbon emission across different geographical regions (first two rows) and commodity groups (last three rows) over the period between 2005-2021. Thick lines denote group aggregates, while thin lines trace the select country- or commodity-level changes. The selected countries and commodities have their amortised deforestation > 0.5% of total amortised deforestation globally and non-overlapping temporal trends from their respective groups. For this trend analysis, we use the amortised results to minimise inter-annual variability and visualise clear temporal trends – showcasing relative change to the baseline year 2005.

1.3 Comparison and quality assessment

Comparing DeDuCE's estimates with existing datasets, we observe nearly similar trends, albeit with some variations in their overall magnitude (Fig. 5). DeDuCE reports higher deforestation estimates due to its extensive coverage of countries and commodities, surpassing previous studies that were limited to either tropical deforestation[9] or a select group of major deforestation commodities[10] (Fig. 5a,b). An instance where our deforestation estimates are lower than ref. [13] (Fig. 5a), the difference is likely due to them considering rotational clearing as deforestation. This could inflate deforestation estimates by 20-35% (Fig. 2). A similar pattern is observed while comparing our carbon emissions estimates with ref.[46] (Fig. 5b). This is mainly because their methodology also does not distinguish between rotational clearing and deforestation, nor does it factor in potential carbon sequestration resulting from land-use changes (i.e., land use replacing forest).

When examining the comparative trends between EUDR and staple commodities (Fig. 5c-l), we observed that our deforestation estimates for cocoa, rubber and forest plantations vary from those in previous studies[9,10] (Fig 5e,f). Despite these discrepancies, we contend that employing spatial datasets to attribute these commodities[18,19,21] to deforestation should yield more accurate estimates than those relying solely on agricultural and forestry statistics[25].

Assessing the quality of our model's deforestation estimates unveils intriguing insights (Fig. 6). Notably, nearly 20% of the total deforestation estimates are derived from spatial attribution using commodity-specific remotely sensed datasets, earning the highest quality score (Fig. 6a). Conversely, the subsequent 30-35% of the attribution combines spatial assessments broad land-use expansions leading to deforestation with agricultural statistics, integrating both spatial and statistical attribution methods. The remaining 50-55% is derived by blending probable estimates of major drivers with agricultural statistics, mainly through statistical deforestation attribution (Fig. 6a). Within these statistical attributions, sub-national agricultural statistics receive the highest scores, followed by national official and then imputed values, with the lowest scores given to estimates gap-filled by our study. High-quality scores are particularly notable in South America and Southeast Asia (Fig. 6b,c), and for commodities like oil palm, soya beans, rubber, and cocoa, due to better spatial data availability (Fig. 6d,e). This analysis not only affirms the accuracy of attribution estimates but also points out data gaps for other key deforestation-risk commodities worldwide (e.g., maize in the DR Congo or cocoa in Indonesia; Supplementary Fig. 3).

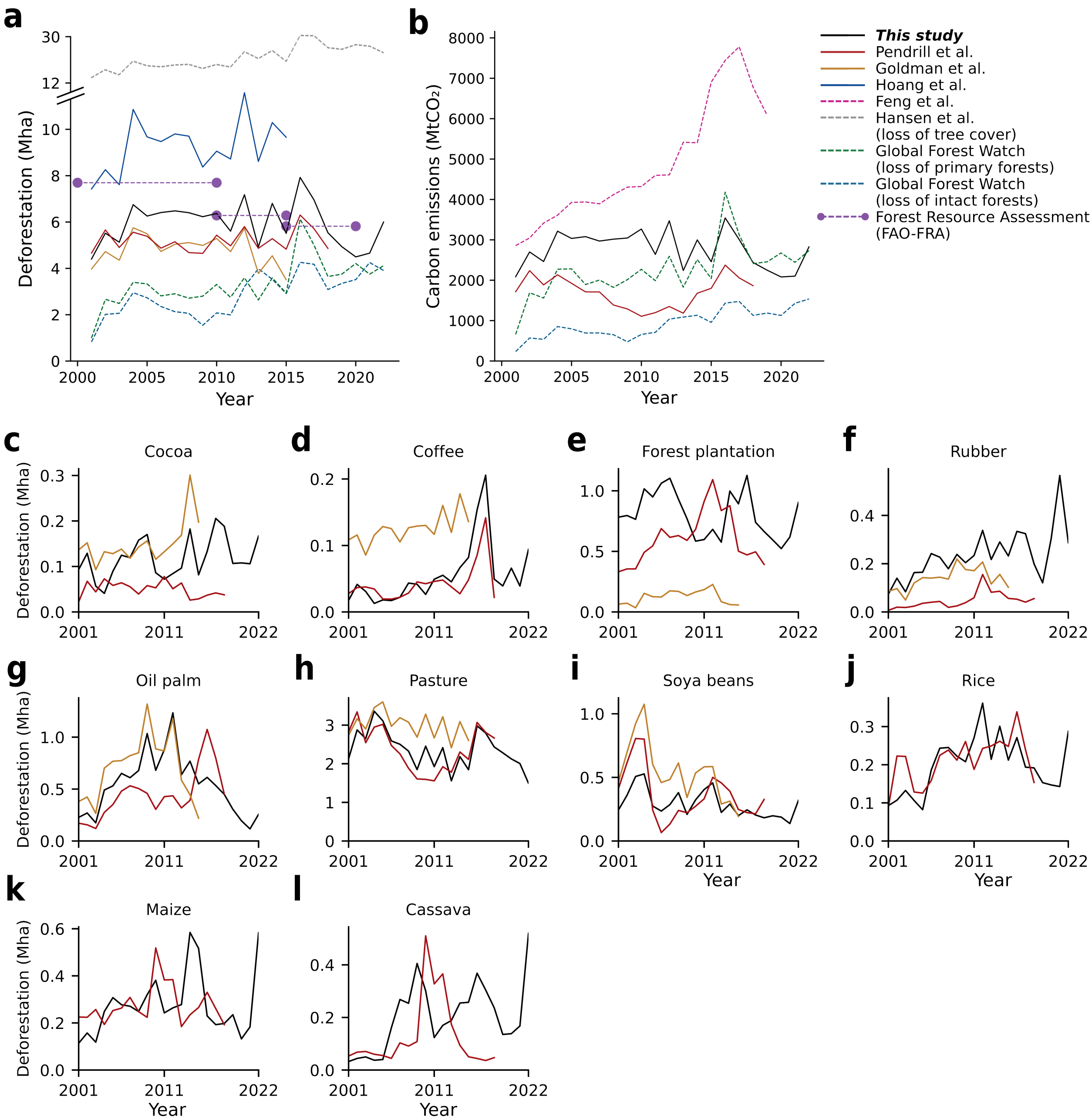

Fig. 5 | Comparing different commodity-driven deforestation estimates. Here, we present a comprehensive comparison between our (a) deforestation and (b) associated carbon emission estimates (excluding peatland emissions) with those from established literature sources. The comparison is facilitated using estimates from Pendrill et al.[9], Goldman et al.[10], Hoang et al.[13], Feng et al.[46] (only including commodity-driven deforestation), Hansen et al.[15] (tree cover ≥ 25%), Global Forest Watch[47] (tree cover ≥ 25%) and FAO's global forest resource assessment report (FAO-FRA)[2]. Furthermore, the figure delves into the comparison of deforestation estimates for (c-i) commodities under the European Union Deforestation Regulation (EUDR) framework and (j-l) major staple commodities.

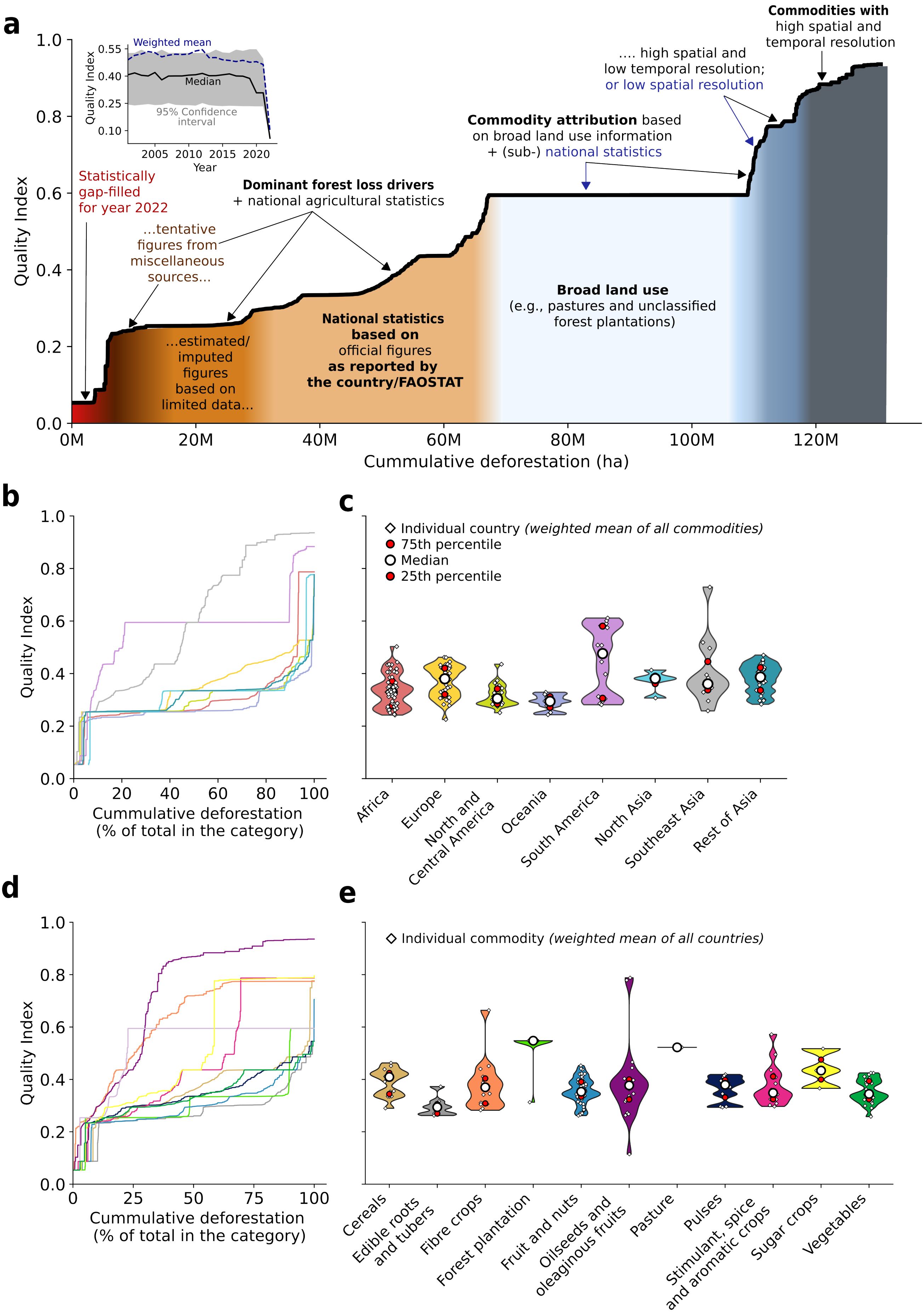
a
Quality Index
Cummulative deforestation (ha)
0M
20M
40M
60M
80M
100M
120M
Weighted mean
Median
95% Confidence interval
Year
Statistically gap-filled for year 2022
...tentative figures from miscellaneous sources...
Dominant forest loss drivers + national agricultural statistics
...estimated/ imputed figures based on limited data...
National statistics based on official figures as reported by the country/FAOSTAT
Broad land use (e.g., pastures and unclassified forest plantations)
Commodity attribution based on broad land use information + (sub-) national statistics
.... high spatial and low temporal resolution; or low spatial resolution
Commodities with high spatial and temporal resolution
b
Cummulative deforestation (% of total in the category)
c
Individual country (weighted mean of all commodities)
75th percentile
Median
25th percentile
Africa
Europe
North and Central America
Oceania
South America
North Asia
Southeast Asia
Rest of Asia
d
e
Individual commodity (weighted mean of all countries)
Cereals
Edible roots and tubers
Fibre crops
Forest plantation
Fruit and nuts
Oilseeds and oleaginous fruits
Pasture
Pulses
Stimulant, spice and aromatic crops
Sugar crops
Vegetables

311

Fig. 6 | Evaluating the quality of commodity-driven deforestation estimates. (a) The ranked line plot visualises the quality index score of deforestation estimates for different country-commodity pairs, arranged from the lowest quality index score (on the left) to the highest (on the right). The insets (in a) provide insights into the data types and their level of explicitness, which contribute to the respective quality index rankings. (b,d) A similar analysis is replicated for distinct geographical regions and commodity groups. (c,e) Violin plots depict the weighted mean quality scores across these regions and groups, with their width representing the number of countries or commodities at respective quality indexes. The colour scheme for geographical regions (in b,c) and commodity groups (in d,e) is the same as in Fig. 3.

1.4 Future improvements to the model

The DeDuCE model – leveraging remote sensing and agricultural statistics – marks a leap forward in deforestation attribution and assessment of carbon emissions for agricultural and forestry commodities. Its effectiveness, however, depends on the quality and availability of data. Thus, as better and more granular data becomes available for regions with poor spatio-temporal representation, the precision of our model will also improve.

Our prediction about the future potential of the DeDuCE model is anchored in the burgeoning field of remote sensing technology. With satellite datasets achieving higher resolutions and the integration of sophisticated statistical methods, including machine learning and temporal trend analysis techniques, the model's data sources are set to become more robust. This will enable enhanced detection of inter- and multi-cropping patterns, more accurate phenological mapping of both temporary and perennial crops, more precise differentiation between managed and natural forests, and better synchronisation of deforestation events with productive agricultural activities. However, such enhancements are limited by the need for extensive field data for model training, particularly outside well-studied regions. In such cases, integrating sub-national agricultural statistics can further refine the model's estimates, providing a more nuanced understanding of how agricultural trends contribute to deforestation. Furthermore, EUDR and similar policies may provide essential data for model validation and refinement.

For carbon emissions, future work will focus on improving estimates of soil organic carbon (SOC) losses and the plant carbon stocks of replacing commodities, by incorporating more detailed geographic and commodity-specific data.

These improvements will not only refine our deforestation and emission estimates, but will also expand the scientific and practical utility of our model. For instance, the results of the DeDuCE model can facilitate a nuanced approach for governments engaged in consumption-based deforestation and emissions accounting, enabling the formulation of policies that more accurately reflect the environmental costs of domestic consumption. This is essential for countries committed to fulfilling international climate commitments and adopting effective land-use strategies that simultaneously reduce carbon emissions and foster sustainable development. Additionally, companies aiming for deforestation-free supply chains can pinpoint their region of operations that might be causing environmental harm, allowing them to adopt more sustainable practices proactively. Based on this, the DeDuCE model can serve as a conduit between data and actionable insights for a broad spectrum of stakeholders, each playing a crucial role in the collective effort to combat deforestation and its global implications.

2. Methods

The DeDuCE model leverages a comprehensive array of spatial and agricultural census data to accurately quantify deforestation and the associated carbon emissions from agricultural and forestry activities. The model framework involves three primary steps (Fig. 1): (i) *Deforestation attribution*, categorised into spatial and statistical attribution, pinpoints the locations (wherever possible) and extent of forest loss attributable to agriculture and forestry commodities. By superimposing multiple datasets on forest loss pixels, each with varying degrees of scope and detail, we aim to capture the most comprehensive information possible regarding the drivers of forest loss. (ii) *Carbon emission calculation* assesses the carbon emissions generated from deforestation linked to agriculture and forestry commodities, including additional emissions from deforestation in peatlands (through peatland drainage). (iii) *Quality assessment or flagging* scrutinises the reliability of our deforestation estimates by examining the quality of the input data and its incorporation into the model (Fig. 1). The model generates annual deforestation and carbon emission estimates, along with a quality index for each country-commodity pairing at national level (and sub-national level for Brazil), adhering to the administrative boundaries defined by the Database of Global Administrative Areas (GADM) version 4.1[48]. Detailed information on the datasets used in this model is presented in Supplementary Table 3.

2.1 Deforestation attribution

To assess the contribution of agricultural and forestry activities to annual deforestation, we overlay different land-use products that demarcate cropland[20], forest plantation[21] and pasture extents[22], crop commodity such as soybeans[16] and cocoa[18], and drivers of forest loss like fire[49] and shifting agriculture[21], on an annual tree cover loss dataset[15] spanning from 2001 to 2022 (Fig. 1). Spatial attribution directly utilises a wealth of remote sensing data to allocate tree cover loss to either specific commodities (e.g., soybeans or oil palms), specific land-uses (e.g., croplands, pastures, forest plantations, or mixed land-use mosaics), or broad deforestation drivers (e.g., commodity-driven deforestation or forestry activities), depending on the availability of spatial data (Fig. 1). Where the proximate cause of deforestation is not attributable to a single commodity via spatial analysis, we employ statistical attribution using FAOSTAT's and Forest Resource Assessment (FRA) annual land use and commodity production statistics[2,25] to attribute deforestation to specific commodities (Fig. 1).

2.1.1 Spatial attribution

In this step, we commence by evaluating annual tree cover loss using the global forest change dataset[15] as a foundational layer (Fig. 1). This dataset defines tree cover based on the presence of woody vegetation exceeding 5m in height within each 30m pixel. Recognising that not all woody vegetation constitutes natural forest, we adopt a tree cover density threshold of ≥25% per pixel to delineate forested areas, a standard threshold adapted from previous studies[12,50–52]. Pixels meeting this threshold are classified as forest, while those falling below are considered non-forest and are not included in subsequent forest loss assessments. It's important to note that while we initially apply this ≥25% tree cover density threshold, our DeDuCE model is designed with the flexibility to adjust this threshold as needed to suit varying definitions of forest cover.

We then overlay the forest loss layer with a diverse set of spatial datasets to gain insights into (i) whether a given pixel of forest loss constitutes deforestation and (ii) what was the proximate cause of that deforestation. To ensure a coherent integration of this data, we employ a hierarchical attribution based on a scoring system that evaluates each dataset's relevance based on spatial coverage, temporal frequency, and the specificity of deforestation driver and causation (i.e., explicitness) (Supplementary Table 4). Further particulars of this scoring system are delineated in the

'Quality assessment' subsection below, but for each forest loss pixel, we prioritise the most detailed information on the direct cause of forest loss. This means that we prioritise spatial data on specific agricultural commodities, then broader land use categories, and finally general or dominant forest loss drivers. Whenever datasets overlap in content (similar land use or commodity), those with higher spatio-temporal resolution take precedence. Furthermore, our model refrains from attributing forest loss to spatial data beyond the most recent year of available information, ensuring that our analysis reflects the latest land use status. This approach ensures that once a pixel's forest loss is accounted for, it is no longer considered in the further attribution process.

We process temporally explicit datasets, like MapBiomas and Soybeans, which offer yearly spatial extent from 2000 to 2022, differently from those that are temporally aggregated. Temporally explicit datasets facilitate direct attribution of deforestation to particular land-uses or commodities. We process them by applying a four-year moving window (i.e., a maximum three-year delay) from the year of detected forest loss. This window helps compensate for any delays between the observed forest loss and the actual conversion of that deforested land to an agricultural land use. For instance, if a pixel shows forest loss in 2001 and is later identified as cropland in 2003 by MapBiomas, we attribute that forest loss to cropland. In cases where multiple land-use changes occur within the window, we prioritise the assignment in the order of forest plantations, woody perennial crops, pastures, herbaceous perennial and temporary crops (thus prioritising land-uses with higher rotation period over lower[53,54]).

Conversely, datasets that aggregate data over time pose challenges in pinpointing the immediate cause of deforestation, as they may not capture sequential land-use changes. Taking the cocoa plantations dataset as an example[18], which consolidates satellite data from 2018 to 2021 into a single reference year, we may risk misidentifying the deforestation driver if land use has varied within the intervening years. In such cases, if there is an overlap of cocoa plantation areas with forest loss pixels from 2003 and no intervening land use data present between 2003-2017, it is challenging to ascertain whether cocoa cultivation is a direct or indirect deforestation driver. Here, we follow a simplistic approach by aligning these temporally aggregated datasets with the year of forest loss when spatial overlap occurs (i.e., simply assuming that the land use that is eventually identified represents the proximate cause of deforestation). However, the attribution of forest loss does not extend beyond the year of detection.

Next, we filter out the loss of managed forests (i.e., both planted and plantation forests; see definition at ref.[2]) from our deforestation attribution, focusing solely on the loss of natural forests. Since the global forest change dataset[15] does not differentiate between natural and managed forests, recognising any woody vegetation over 5m in height in a pixel as forested land, the signal from forest loss contains both removal of tree stands in natural forests (i.e., deforestation) and managed forests (due to logging and rotation harvesting in already established timber or oil palm plantation regions). To refine our analysis to only include deforestation, we exclude changes in tree cover associated with the management activities of planted and plantation forests established before 2001.

For datasets with annual updates, such as MapBiomas[22] and oil palm extent in Indonesia[17], which document land use since 2000 or earlier, we can readily discern whether land-use changes occur in natural or managed forests. For those without such temporal land-use detail, we employ a forest plantation mask based on Du et al.[21] and Lesiv et al.[24] to identify and exclude managed forests (Supplementary Fig. 5). Du et al.[21] use the Spatial Database of Planted Trees (SDPT version 1.0[55]) – which is stated to cover nearly 82% of plantation forests globally – and time-series of Landsat satellite data (from 1982-2020) to detect when these plantations in a pixel were established. Conversely, Lesiv et al.[24] offer a global perspective on managed forests using more recent satellite imagery (2014-2016) and expert classification.

When pixels corresponding to forest plantations or tree crops (e.g., oil palm, coconut, and cocoa), those lacking a land-use record for the year 2000, intersect with the forest plantation mask (Supplementary Fig. 5), we consider these pixels to have been established pre-2001 and exclude them from our deforestation attribution analysis. We give precedence to Du et al.[21] plantation mask due to its comprehensive temporal coverage, which allows us to distinguish between natural and manged forest cover changes before and after the year 2000. In regions without coverage from Du et al.[21], such as Canada and Russia, we defer to Lesiv et al.[24] plantation mask. The latter case, however, may lead to conservative estimates of deforestation where plantation expansion occurred between 2001-2016 (since Lesiv et al.[24] is defined using remote sensing data from 2014-16), but the impact on our overall results is deemed minimal given the breadth of the SDPT database[55]. This masking is selectively applied to forest plantations and tree crops commodities; temporary crop and pasture commodities, typically non-woody and less likely to replace forest plantations, are not subjected to this masking.

In the final step of the spatial attribution, we address forest loss resulting from fires, a natural process crucial for ecological equilibrium, particularly in boreal regions. We systematically remove fire-related forest loss from our deforestation attribution, using spatio-temporal data[49] that identifies such events. Additionally, for regions not captured by the commodity and land-use datasets listed in Supplementary Table 3, we employ a global dataset by Curtis et al.[23] that identifies the dominant drivers of forest loss (supplemented with the global forest plantation mask to segregate natural forest loss from the loss over managed forests post the year 2000; Supplementary Fig. 5). All preprocessing methodologies applied to these spatial datasets are detailed in Supplementary Table 5.

The result of the spatial attribution is a dataset that summarises at the (sub-)national level, the amount of deforestation attributed to specific commodities and land-uses (croplands, pastures, or forest plantations), as well as mosaics of multiple land-use and deforestation drivers (Fig. 1). The entire process of spatial deforestation attribution, involving the analysis of terabytes of spatial data, is conducted utilising Google Earth Engine.

2.1.2 Statistical attribution

Despite spatial attribution, considerable deforestation remains unclassified to specific commodities. This occurs for three main reasons: (i) when we have specific land-use information indicating the cause of deforestation is either a cropland, pasture or forest plantation; (ii) the presence of land-use mosaics, specifically the MapBiomas[22] dataset, which identifies pixels as a cropland and pasture mosaic when the algorithm cannot distinctly separate the two, or the Curtis et al.[8] dataset, which determines the primary driver of forest loss aggregated over a 22-year period; or (iii) instances where forest loss is not linked to any specific commodity or land-use by the existing spatial datasets (Supplementary Table 3). To address the ambiguity in the latter two cases and attribute forest loss to a specific commodity, we follow a two-step statistical land-balance approach (adapted from ref.[12]).

In this two-step statistical attribution (Supplementary Fig. 6), we first attribute deforestation (from the latter two cases) to either cropland ($FL_{CL,statistical,t}$), pasture ($FL_{PP,statistical,t}$), or forest plantations ($FL_{FP,statistical,t}$). This method utilises annual land use data from FAOSTAT[25] and FRA[2] to inform on the extent of land-use expansion in these indeterminate areas of deforestation (referred to as 'statistical land-use attribution' in Fig. 1). Building on these land-use expansions, we further attribute cropland deforestation to various crop commodities according to their respective increases in harvested area (again using FAOSTAT[25]; referred to as 'statistical commodity attribution' in Fig. 1 and Supplementary Fig. 6). Similarly, deforestation from pasture expansion is linked to cattle meat and leather products.

We directly attribute deforestation resulting from forest plantations to forestry products due to the absence of detailed forestry-commodity information.

We start the first step of this statistical attribution by estimating the expansion of croplands (*CLE*), permanent pastures (*PPE*), and forest plantations (*FPE*) over a three-year time lag following the observed year of forest loss (*t*), such that *lag* = min {3, 2022 – *t*} (Eq. 1-3; Supplementary Fig. 6). The duration of this lag period is set to three years, reflecting empirical data on the typical interval between the initial forest clearing and the subsequent establishment of agricultural land for production[56,57]. This time-lagged approach is integral to synchronising the observed changes in land cover with the likely temporal dynamics of land-use development.

$$CLE_t = \max\left\{\frac{\left(CL_{t+lag} - CL_t\right) + \sum_{t}^{t+lag} Crop\ loss_t}{lag} - GPL_t, 0\right\};\ GPL_t = \max\left\{\min\left\{\frac{\left(PP_{t+lag} - PP_t\right)}{lag}, \frac{\sum_{t}^{t+lag} Grass\ loss_t}{lag}\right\}, 0\right\} \quad (1)$$

$$PPE_t = \max\left\{\frac{\left(PP_{t+lag} - PP_t\right) + \sum_{t}^{t+lag} Grassloss_t}{lag}, 0\right\} \quad (2)$$

$$FPE_t = \max\left\{\frac{FP_{t+lag} - FP_t}{lag}, 0\right\} \quad (3)$$

Here CL_t, PP_t, FP_t quantify the extent of croplands, permanent pastures, and forest plantations for a given year *t*, respectively. The land-use extent data for croplands and permanent pastures are sourced from FAOSTAT[25] (Eq. 1-2), while information on forest plantations is obtained from the FRA[2] (Eq. 3). Our analysis is focused on gross land-use change; hence, we enhance the net expansion figures from FAOSTAT and FRA with estimates of crop and pasture loss. These losses are computed using methodologies from Li et al.[58], which utilise a time series of the ESA CCI land cover dataset[59] (2000-2020; gap-filling by averaging the estimates for the last two years) to track changes in crop and grass areas (i.e., proxy for pasture loss area).

Acknowledging the frequent expansions of croplands over pastures, as evidenced by remote sensing studies[36], we adjust our cropland expansion (CLE_t) calculations by deducting the gross pasture loss (GPL_t) (Eq. 1). This reflects the tendency for croplands to expand initially into pasture areas before encroaching on forested lands. This displaces cattle ranching into forest frontiers due to cropland expansion[12,60], leading us to correlate pasture expansion directly with forest loss (Eq. 2). In contrast, for forest plantations, we account only for the net change, as data on gross plantation loss is not available. Consequently, the expansion of forest plantations is directly linked to forest loss (Eq. 3).

When faced with multi-land-use mosaics (specifically for MapBiomas[22], Curtis et al.[8] dominant driver dataset, and unclassified forest loss) that blend croplands, pastures, or forest plantations without clear demarcation, we distribute the area of forest loss within these mosaics (FL_{mosaic}) in proportion to the extent of each land use relative to the total observed expansion of land use (Eq. 4-6; Supplementary Fig. 6). This means that the mosaic of cropland, pasture, and forest plantation is divided among them based on their respective contributions to overall land use expansion (i.e., the sum of CLE_t, PPE_t and FPE_t) (Eq. 4-6). In scenarios where the mosaic is solely composed of cropland and pasture (presently only MapBiomas[22]), we allocate the area between these two categories proportionately, with the combined extent of CLE_t and PPE_t – informing the total area used for this allocation.

$$FL_{CL,statistical,t} = \underset{(certain)}{FL_{mosaic,t}} \times \frac{CLE_t}{CLE_t + PPE_t + FPE_t} \quad \text{or} \quad \min\left\{\max\left\{CLE_t - FL_{CL,spatial,t}, 0\right\}, \underset{(uncertain)}{FL_{mosaic,t}} \times \frac{CLE_t}{CLE_t + PPE_t + FPE_t}\right\} \quad (4)$$

$$FL_{PP,statistical,t} = \underset{(certain)}{FL_{mosaic,t}} \times \frac{PPE_t}{CLE_t + PPE_t + FPE_t} \quad \text{or} \quad \min\left\{ \max\left\{PPE_t - FL_{PP,spatial,t}, 0\right\}, \underset{(uncertain)}{FL_{mosaic,t}} \times \frac{PPE_t}{CLE_t + PPE_t + FPE_t} \right\} \tag{5}$$

$$FL^{'}_{FP,statistical,t} = \underset{(certain)}{FL_{mosaic,t}} \times \frac{FPE_t}{CLE_t + PPE_t + FPE_t} \quad \text{or} \quad \min\left\{ \max\left\{FPE_t - FL_{FP,spatial,t}, 0\right\}, \underset{(uncertain)}{FL_{mosaic,t}} \times \frac{FPE_t}{CLE_t + PPE_t + FPE_t} \right\} \tag{6}$$

In this framework, mosaics are also divided into 'certain' and 'uncertain' categories. 'Certain' mosaics are those where the dataset confidently identifies the type of land use within the mosaics. For instance, MapBiomas[22] mosaics are certain that the mosaic land use is either a cropland or pasture. Conversely, 'uncertain' mosaics, specifically those from the Curtis et al.[23] dataset, suggest probable land uses solely based on the predominant cause of forest loss over space and time, which may not always accurately reflect direct drivers of forest loss (since aggregated in a 10-km pixel over the full time period). This also encompasses unclassified forest loss as well, given that the driver of such forest loss cannot be associated with a specific land use. We impose a limit for these ambiguous cases (i.e., uncertain mosaics) (Eq. 4-6). This constrains the categorisation of forest loss to whichever is smaller: the expansion of land-use categories minus the spatially attributed forest loss or the forest loss proportionally assessed based on relative land-use expansions – to avoid overestimating forest loss due to agriculture.

Additionally, despite using a forest plantation mask, certain areas might inaccurately identify themselves as forest loss within natural forest, when in reality, they represent rotational clearing. This misclassification is particularly prevalent when forest loss pixels coincide with areas identified by Curtis et al.[23] as forestry-driven deforestation ($FL_{forestry,spatial,t}$), stemming from challenges in differentiating between natural and managed forest losses. This issue is especially notable in countries like Sweden, Canada, and Russia, where extensively managed forest areas are not categorised as plantation forests according to FAO's definitions. To counter potential overestimation of deforestation driven by forestry activities, our methodology enforces a cap on the statistical accounting of forest loss attributed to forest plantations ($FL^{'}_{FP,statistical,t}$). This cap ensures that the reported forest loss does not surpass the forest plantation expansion estimates provided by the FRA (i.e., *FPE_t*; Eq. 7).

$$FL_{FP,statistical,t} = \begin{cases} FL^{'}_{FP,statistical,t} & \text{if } FL_{forestry,spatial,t} > 0 \text{ and } \\ & FPE_t \le FL_{FP,spatial,t} + FL^{'}_{FP,statistical,t} \\ \min\left\{FPE_t - FL_{FP,spatial,t}, FL_{forestry,spatial,t} + FL^{'}_{FP,statistical,t}\right\} & \text{if } FL_{forestry,spatial,t} > 0 \text{ and } \\ & FPE_t > FL_{FP,spatial,t} + FL^{'}_{FP,statistical,t} \end{cases} \tag{7}$$

It should be noted that FAOSTAT provides land-use data up to the year 2021, which allows us to compute land-use expansion until 2020 (Eq. 4-6). To gap-fill for expansions in 2021 and 2022, we average the land use expansion from the preceding three years (i.e., 2018-2020) and then adjust it proportionally to the forest loss to estimates of 2021 and 2022 (Eq. 8).

$$CLE_t = \min\left\{ \overline{\sum_{i=t-3}^{t-1} CLE_i},\ \overline{\sum_{i=t-3}^{t-1} CLE_i} \times \frac{FL_t}{\overline{\sum_{i=t-3}^{t-1} FL_{CL,i}}} \right\} \qquad PPE_t = \min\left\{ \overline{\sum_{i=t-3}^{t-1} PPE_i},\ \overline{\sum_{i=t-3}^{t-1} PPE_i} \times \frac{FL_t}{\overline{\sum_{i=t-3}^{t-1} FL_{PP,i}}} \right\}$$
$$FPE_t = \min\left\{ \overline{\sum_{i=t-3}^{t-1} FPE_i},\ \overline{\sum_{i=t-3}^{t-1} FPE_i} \times \frac{FL_t}{\overline{\sum_{i=t-3}^{t-1} FL_{FP,i}}} \right\} \tag{8}$$

In addition, due to FAO's methodology of consolidating land use statistics, certain countries that have undergone political changes are treated as single units for our analysis. For instance, Sudan and South Sudan's data are merged and presented under the unified label of 'Sudan'. Similarly, Serbia and Montenegro are too combined for our land use calculations, and the results are reported under 'Serbia'. This approach ensures consistency with the FAO's data aggregation practices and enables a coherent analysis of land use trends over time in our modelling framework.

In the second-step of statistical attribution (Supplementary Fig. 6), we allocate total forest loss induced by cropland expansion ($FL_{CL,t}$, which is the sum of deforestation attributed to croplands spatially and statistically) to various crop commodities ($FL_{CL,statistical,i,t}$, where *i* refers to individual commodities). After excluding forest loss due to commodities already accounted for spatially ($\sum_i FL_{CL,spatial,i,t}$),the statistical land-use attribution step (Eq. 9) allocates cropland deforestation proportionally to the expansion of each crop commodity ($CLE_{i,t}$) relative to the total expansion at the country level ($\sum_i CLE_{i,t}$). We use FAOSTAT's country scale 'crops and livestock products' statistics ($CL_{i,t}$) to estimate these expansions[25], maintaining the methodology and lag used previously (Eq. 10). The only exception is Brazil, where we use municipality-level (i.e., second-level administrative boundary) data from the Brazilian Institute of Geography and Statistics (IBGE)[61]. Notably, IBGE also estimates harvested areas for certain crops – specifically maize, groundnuts, potatoes, and beans – that are planted multiple times annually. To prevent double or triple counting of the deforestation attributable to these crops, we only use their first harvested area estimates rather than the total cumulative harvested area over the year. We note that currently, our focus is limited to Brazil due to the poor quality of sub-national statistics in other countries. However, we anticipate incorporating these statistics in the future, as higher-quality data becomes available.

If FAOSTAT or IBGE's total crop expansion ($\sum_i CLE_{i,t}$) exceeds the forest loss attributed to cropland ($FL_{CL,t}$; Eq. 1), we use the lower value between the two (Eq. 9). Additionally, any surplus ($FL_{CL,surplus,t}$) is apportioned among commodities based on their annual harvested areas, preserving proportionality and reflecting possible land-use changes (Eq. 11-12).

$$FL_{CL,statistical,i,t} = \left(\left(\max\left\{ \min\left\{ FL_{CL,t},\ \sum_i CLE_{i,t} \right\} - \sum_i FL_{CL,spatial,i,t}, 0 \right\} \right) \times \frac{CLE_{i,t}}{\left(\sum_i CLE_{i,t} - \sum_j CLE_{j,t} \right)} \right) + FL_{CL,surplus,i,t} \tag{9}$$

$$CLE_{i,t} = \max\left\{ \frac{CL_{i,t+lag} - CL_{i,t}}{lag}, 0 \right\} \tag{10}$$

$$FL_{CL,surplus,t} = FL_{CL,t} - \left(\max\left\{ \min\left\{ FL_{CL,t},\ \sum_i CLE_{i,t} \right\} - \sum_j FL_{CL,spatial,i,t}, 0 \right\} \right) - \sum_j FL_{CL,spatial,i,t} \qquad if\ \ FL_{CL,t} > \sum_i CLE_{i,t} \tag{11}$$

$$FL_{CL,surplus,i,t} = FL_{CL,surplus,t} \times \frac{CL_{i,t}}{\sum_{i} CL_{i,t}} \tag{12}$$

Here, $\sum FL_{CL,spatial,i,t}$ is the sum of all spatially attributed forest loss commodities. Since we prioritise deforestation estimated through remote sensing data over agricultural statistics, spatially attributed commodities with a score greater than 0.85 are excluded from statistical attribution. This threshold indicates a high confidence in the data reflecting the true extent of deforestation by that commodity, such as soybeans in South America and oil palm in Indonesia (scores for all datasets are mentioned in Supplementary Table 4, with the scoring methodology outlined in the 'Quality assessment' section). To compensate for this exclusion, we adjust the total crop commodity expansion by deducting $\sum_{j} CLE_{j,t}$ (i.e., the sum of harvested areas of commodities scoring above 0.85 or $FL_{CL,spatial,i,t} > CLE_{i,t}$) from $\sum_{i} CLE_{i,t}$ (Eq. 10). Additionally, as FAOSTAT provides harvest area data up to 2021, enabling commodity-driven expansions calculation up to 2020, we apply a similar methodology as before gap-fill for the year 2021 and 2022 (Eq. 4-6).

We would also like to highlight that the year 2022 deforestation estimates for Brazil present a suboptimal case of gap-filling (Eq. 8), resulting in an unrealistic surge in crop commodity-driven deforestation (Supplementary Fig. 7). This surge is largely due to the spatial attribution approach, primarily led by the use of Curtis et al.[8] dominant driver of forest loss data for year 2022, diverging from the MapBiomas[22]-led attribution in earlier years, resulting in a higher deforested land-use allocation to croplands and pastures (under combined allocation to commodity-driven deforestation class in Curtis et al.[8]; Fig. 1 and Supplementary Fig. 7a). The inconsistency is further exacerbated for crop commodities due to the integration of agricultural statistics at varying administrative levels. Specifically, while IBGE offers commodity production data at the subnational level (used for commodity expansion calculation in Eq. 9), it lacks corresponding land-use (cropland, pasture, and forest plantations) statistics at the subnational level (for assessing statistical land-use attribution; Fig. 1). Consequently, we have to rely on FAOSTAT's national-level land-use statistics to estimate CLE_{2022} and deforestation attributed to croplands ($FL_{CL,statistical,2022}$) at sub-national level (Eq. 1 and 4), which inflates crop commodity-driven deforestation estimates, but underestimates pasture-driven deforestation, as it does not capture sub-national cropland and pasture dynamics (Supplementary Fig. 7b). This discrepancy will be addressed when the year 2022 data for MapBiomas becomes available. Therefore, we recommend exercising caution when interpreting these gap-filled estimates for Brazil for the year 2022. In such instances, utilising the amortised deforestation estimates is advisable, as detailed later in this subsection.

In the case of forest loss due to pastures ($FL_{PP,t}$), we attribute these losses to just two commodities: cattle meat and leather at 95% and 5% of the total deforested area, respectively, based on an economic allocation logic[9]. Although some studies have utilised weighted cattle density data to minimise the inclusion of pastures used for other grazing livestock (e.g., sheep and goats)[10], significant uncertainties remain. For instance, for some countries, the impact on pastoral communities could be considerable, however, the traditional land use and grazing patterns of these communities may diverge from what is detectable through satellite imagery or fit within formal land-use classifications. Moreover, the variability in cattle density over time poses a challenge, and therefore, is difficult to capture with datasets aggregated temporally, which might lead to under- or over-estimation of cattle meat-driven deforestation. As a result, we adopted an approach grounded in economic-allocation logic to attribute commodities to pastures[9].

Forest loss attributed to forest plantations ($FL_{FP,t}$) is categorised as 'Forest plantation (Unclassified)', unless the specific species of the plantations can be spatially attributed using the global plantation dataset[21]. In these cases, where the species information is available, the forest plantation is referred to as 'Forest plantation (*species name*)'.

Besides providing annual (i.e., unamortised) deforestation estimates for country-commodity pairing, we also present amortised deforestation estimates. In environmental impact assessments, particularly regarding deforestation for agricultural purposes, it's crucial to consider not just the immediate impact of forest loss, but also the extended effects of this transformation[9]. The 'amortisation' period conceptually spreads the consequences of deforestation across multiple years to account for the enduring productivity of the land. Hence, when we attribute deforestation to agricultural and forestry commodities, we distribute this attribution evenly over a 5-year amortisation period (similar to a 5-year moving average). This method acknowledges that once the land is cleared, it continues to yield crops annually, and thus, the initial deforestation's footprint is prorated over a period that reflects the ongoing impact of land-use change. This amortisation aligns the temporal scale of deforestation's impact with the timeframe of agricultural production, offering a more nuanced understanding of the long-term ecological footprint of crop cultivation and forestry[62,63].

2.2 Carbon emissions

To calculate carbon emissions, excluding those from peatland drainage, we assess changes in carbon stocks due to forest loss. Our analysis concentrates on five key stocks: aboveground biomass (AGB), belowground biomass (BGB), dead wood, litter and soil organic carbon (SOC) (Fig. 1). Notably, belowground biomass and soil organic carbon losses are typically delayed responses to aboveground disturbances[46]. However, for the purpose of our analysis, these losses are treated as if they are an inevitable consequence of the deforestation, often referred to as 'one-off' or 'committed' losses. Essentially, it implies that once a region is deforested, the belowground carbon and associated SOC is also considered lost, even though it might happen slowly over time.

AGB per pixel (in Mg px^{-1}) is derived from the aboveground live biomass density data for year 2000 at 30-m resolution[26]. Based on this AGB, BGB is spatially estimated using a root-to-shoot ratio (i.e., BGB/AGB ratio) from ref.[64] across various biomes[65] (Supplementary Table 6). Dead wood and litter biomass densities are also spatially calculated as proportions of AGB, informed by biome-specific lookup tables that factor in elevation and precipitation (lookup table in ref.[26]). These biomass densities are converted to carbon densities (i.e., MgC px^{-1}) using a standard biomass-to-carbon conversion ratio of 0.47 for forest ecosystems, as recommended by the IPCC[66].

We commence by calculating the committed carbon emissions from AGB, BGB, dead wood, and litter. For spatially attributed commodities ($FL_{CL,spatial,i,t}$), carbon emissions are calculated by overlaying forest loss pixels onto the corresponding total carbon stock maps. For statistically attributed commodities ($FL_{CL,statistical,i,t}$), emissions are apportioned based on their proportion to the total forest loss associated with that commodity's land-use ($FL_{CL,statistical,t}$; carbon emissions are also partitioned and aggregated using the same logic as commodity attribution). Hence, if maize's statistically attributed forest loss accounts for 50% of all forest loss from croplands, maize would also bear 50% of the total (statistical) carbon emissions attributed to (statistical) cropland expansions.

Soil organic carbon (SOC) stock data is obtained from the SoilGrids2.0 dataset[27], which provides SOC stocks at varying depths at 250-m resolution (in MgC ha^{-1}). For our purposes, we consider SOC within the top 100cm of soil, the layer most affected by land-use changes, and upscale this data to a 30-m resolution (estimates expressed in MgC px^{-1}). In light of limited data on SOC losses over deforested regions, we adopt an alternative approach informed by meta-analyses – which indicates that converting natural forests to either a cropland, pasture or forest plantation will typically result in decreased SOC stocks. Consequently, we represent the emission from SOC loss as a fraction of the existing SOC stocks for different replacing land use and biome of deforestation (Supplementary Table 7). These emissions from SOC losses are then added to the carbon emissions calculated from AGB, BGB, deadwood and litter, culminating in a comprehensive carbon emission estimate (Eq. 13).

From the emissions outlined above, we deduct the committed carbon sequestration potential of the replacing commodity (e.g., carbon stored as vegetation biomass if the replacing land use is maize or forest plantation) (Eq. 13). This deduction is informed by a meta-analysis of plant carbon stocks across commodities (in MgC ha^{-1}), and categorised into 40 commodities across 11 commodity groups (Supplementary Table 8). If a specific commodity data is absent, we associate it with plant carbon stocks of its respective commodity group (Supplementary Table 2). The resulting net carbon emissions are then expressed in megatonnes of CO_2 ($MtCO_2$). We also amortise these attributed carbon emissions over a 5-year period[9] (reason mentioned in 'Statistical attribution' sub-section).

$$\text{Net carbon emissions} = \text{AGB} + \text{BGB} + \text{Deadwood} + \text{Litter} + \text{SOC loss} - \text{Plant carbon stocks of replacing commodity} \quad (13)$$

2.2.1 Peatland drainage emissions

To align with the deforestation attribution analysis, our model concentrates on carbon emissions from deforestation occurring on peatlands post-2000, deliberately excluding continuous emissions from established agricultural peatlands or those deforested earlier. By superimposing a high-resolution global peatland map (a composite map prepared from multiple sources at 30-m resolution; see ref.[67]) onto identified forest loss, we isolate peatland deforestation linked to specific commodities and land-uses post-2000 (Fig. 1). In the presence of spatial commodity data, overlapping peatland deforestation is directly attributed to the corresponding commodity. In their absence, however, we evenly allocate deforested peatland areas among all identified commodities expansions within a country (similar to forest loss categorisation and commodity attribution).

Assessing emissions from peatland drainage is difficult due to uncertainties in peat subsidence, which can vary with local conditions and management practices. This variability, alongside the inherent challenges in measuring peatland emissions due to the dynamic nature of peat decomposition and water table fluctuations, complicates the accuracy of such estimates. Thus, to assess emissions from peatland drainage, we use emission factors reported by published literature (often represented in $MgCO_2$ ha^{-1} yr^{-1}). These factors are informed by subsidence observations and standardised rates of peat oxidation, providing a scientifically grounded approach to these emission factor calculations[68].

Based in previous meta-analyses of peatland emission factors[68–70] (Supplementary Table 9), we have stratified emission factors by land use expansions (such as peatland drainage due to cropland, pasture or forest plantation expansions; or oil palm expansions specifically) and deforestation biome (i.e., tropical, temperate and boreal), which allows us to apply these factors to specific drainage conditions for different biomes. We multiply these emission factors with peatland drainage area (result expressed in $MgCO_2$ yr^{-1}). Unlike committed emissions, these peatland drainage emissions continue to accumulate, year on year, from the initial deforestation event until the conclusion of our study period. For instance, if a hectare of peatland is cleared and drained for oil palm in 2010 incurs annual emissions of 54.41 $MgCO_2$ every year, this yearly emission persists through to the year 2022, irrespective of subsequent deforestation activities in the interim period.

2.3 Quality assessment

Our methodology, which integrates multiple datasets including spatial extent and agricultural census data, allows us to assess the quality of our deforestation attribution for each country-commodity pairing (Fig. 1). We achieve this by breaking down attributed forest loss ($FL_{i,t}$) for an individual country-commodity pairing (commodity i for year t) into contributions from each data source that led to its aggregation ($FL_{i,j,t}$, where j represents individual data sources), and by factoring in the source-specific overall accuracy of the dataset (OA_j). We recognise that dataset accuracies are relative – while a spatial dataset for cropland and soya beans may both exhibit over 90% accuracy, their precision in pinpointing soya bean cultivation (or deforestation) varies. To standardise quality assessment across datasets, we apply a scoring metric ($Score_j$) that equalises evaluation criteria (Supplementary Table 4), thereby ensuring consistent quality measures specific to the attribution of each commodity (Eq. 14).

$$Quality\ Index_{i,t} = \frac{\sum_{j=1}^{n}\left(FL_{i,j} \times OA_{\mathrm{j}} \times Score_j\right)_t}{FL_{i,t}} \tag{14}$$

Our scoring metric ($Score_j$) hinges on three pivotal (and equally weighted) criteria assessing each dataset's spatial and temporal granularity and explicitness. Spatially, a maximum score (of '1') is assigned to datasets with a resolution finer than or equal to 10-m, tailored to individual countries. Temporally, annual datasets from 2001-2022 for herbaceous crops, and comprehensive data from 2000 or earlier for tree crops and forest plantations, receive the top score. For tree crops and forest plantations, data from the year 2000 or earlier allows us to distinguish post-2000 deforestation from rotational clearing, thus removing the need for plantation mask. For explicitness, datasets mapping a singular commodity, validated by field data, are scored highest. Fluctuating from these conditions, the score of the dataset is penalised. The detailed scoring criteria are mentioned in Supplementary Table 10.

Moreover, as not all commodities are directly attributed through remote sensing datasets but rather inferred statistically by merging remote sensing data with national or subnational agricultural statistics, there arises a need to reflect the reliability of these agricultural statistics in our analysis. To address this, we have refined our scoring metric ($Score_j$) to include data flags from FAOSTAT (Supplementary Table 11), offering a nuanced view of data quality, especially in cases of statistical attribution. In the DeDuCE model's two-step land-balance approach, $Flag_{landuse}$ and $Flag_{production}$ assess the reliability of land-use and commodity expansion data, respectively. We compute the final scoring metric ($Score_j$) by taking the average of these two flags and then integrating it with the score of the remote sensing dataset ($Score_j'$) (Supplementary Table 4; Eq. 15). It is important to note that the IBGE dataset for Brazil does not provide flags for commodity production ($Flag_{production}$). Thus, we assign a default value of '1', reflecting the official figure flag as IBGE directly reports the data.

$$Score_j = Score_j' \times \left(\frac{Flag_{landuse} + Flag_{production}}{2}\right) \tag{15}$$

Data availability: The unamortised and amortised deforestation and carbon emission estimates generated by the DeDuCE model are available on Zenodo: https://doi.org/10.5281/zenodo.10674962. All the datasets used in this study are documented in Supplementary Table 3. The insights from the DeDuCE model can be viewed at: https://www.deforestationfootprint.earth.

Code availability: The Google Earth Engine and Python code for running the DeDuCE model, and those needed to replicate the analysis presented in this study are available at GitHub: https://github.com/chandrakant6492/DeDuCE.

Acknowledgements: C.S. and U.M.P acknowledge the funding support from ÅForsk Foundation (Project name: ReDUCE and grant no.: 22-64) and the Belmont Forum, through FORMAS (Project name: BEDROCK and grant no.: 2022-02563). We also acknowledge the constructive feedback provided by Chris West and Vivian Ribeiro from the Stockholm Environment Institute; and Nancy Harris and Elizabeth Goldman from the World Resources Institute, during various stages of this manuscript's development.

Author contributions: C.S. and U.M.P conceived the study. C.S. led the data analysis, visualisations and writing of the original draft, with substantial feedback from U.M.P. Both authors contributed to interpreting the results and subsequent revisions to the paper.

References

1. FAO. *The State of the World's Forests 2022*. (FAO, Rome, 2022). doi:10.4060/cb9360en.
2. FAO-FRA. Global Forest Resource Assessment 2020. https://fra-data.fao.org/assessments/fra/2020 (2023).
3. Artaxo, P. *et al.* Chapter 23: Impacts of deforestation and climate change on biodiversity, ecological processes, and environmental adaptation. in *Amazon Assessment Report 2021* (eds. Nobre, C. et al.) (UN Sustainable Development Solutions Network (SDSN), 2021). doi:10.55161/VKMN1905.
4. Gomes, V. H. F., Vieira, I. C. G., Salomão, R. P. & ter Steege, H. Amazonian tree species threatened by deforestation and climate change. *Nat. Clim. Chang.* **9**, 547–553 (2019).
5. IPBES. *Global Assessment Report on Biodiversity and Ecosystem Services of the Intergovernmental Science-Policy Platform on Biodiversity and Ecosystem Services*. https://zenodo.org/record/3831673 (2019) doi:10.5281/ZENODO.3831673.
6. Friedlingstein, P. *et al.* Global Carbon Budget 2023. *Earth Syst. Sci. Data* **15**, 5301–5369 (2023).
7. Poore, J. & Nemecek, T. Reducing food's environmental impacts through producers and consumers. *Science* **360**, 987–992 (2018).
8. Pendrill, F. *et al.* Disentangling the numbers behind agriculture-driven tropical deforestation. *Science* **377**, eabm9267 (2022).
9. Pendrill, F. *et al.* Agricultural and forestry trade drives large share of tropical deforestation emissions. *Global Environmental Change* **56**, 1–10 (2019).
10. Goldman, E., Weisse, M., Harris, N. & Schneider, M. Estimating the Role of Seven Commodities in Agriculture-Linked Deforestation: Oil Palm, Soy, Cattle, Wood Fiber, Cocoa, Coffee, and Rubber. *WRIPUB* (2020) doi:10.46830/writn.na.00001.
11. Jin, S. *et al.* National Land Cover Database 2019: A Comprehensive Strategy for Creating the 1986–2019 Forest Disturbance Product. *Journal of Remote Sensing* **3**, 0021 (2023).
12. Pendrill, F., Persson, U. M., Godar, J. & Kastner, T. Deforestation displaced: trade in forest-risk commodities and the prospects for a global forest transition. *Environ. Res. Lett.* **14**, 055003 (2019).
13. Hoang, N. T. & Kanemoto, K. Mapping the deforestation footprint of nations reveals growing threat to tropical forests. *Nat Ecol Evol* **5**, 845–853 (2021).
14. European Union. REGULATION (EU) 2023/1115 OF THE EUROPEAN PARLIAMENT AND OF THE COUNCIL of 31 May 2023 on the making available on the Union market and the export from the Union of certain commodities and products associated with deforestation and forest degradation and repealing Regulation (EU) No 995/2010. https://eur-lex.europa.eu/legal-content/EN/TXT/HTML/?uri=CELEX%3A32023R1115 (2023).
15. Hansen, M. C. *et al.* High-Resolution Global Maps of 21st-Century Forest Cover Change. *Science* **342**, 850–853 (2013).
16. Song, X.-P. *et al.* Massive soybean expansion in South America since 2000 and implications for conservation. *Nat Sustain* 1–9 (2021) doi:10.1038/s41893-021-00729-z.
17. Gaveau, D. L. A. *et al.* Slowing deforestation in Indonesia follows declining oil palm expansion and lower oil prices. *PLOS ONE* **17**, e0266178 (2022).
18. Kalischek, N. *et al.* Cocoa plantations are associated with deforestation in Côte d'Ivoire and Ghana. *Nat Food* **4**, 384–393 (2023).
19. Wang, Y. *et al.* High-resolution maps show that rubber causes substantial deforestation. *Nature* **623**, 340–346 (2023).
20. Potapov, P. *et al.* Global maps of cropland extent and change show accelerated cropland expansion in the twenty-first century. *Nat Food* **3**, 19–28 (2022).

21. Du, Z. *et al.* A global map of planting years of plantations. *Sci Data* **9**, 141 (2022).
22. MapBiomas. *MapBiomas General "Handbook": Algorithm Theoretical Basis Document (ATBD)*. https://mapbiomas-br-site.s3.amazonaws.com/ATBD_Collection_7_v2.pdf (2022).
23. Curtis, P. G., Slay, C. M., Harris, N. L., Tyukavina, A. & Hansen, M. C. Classifying drivers of global forest loss. *Science* **361**, 1108–1111 (2018).
24. Lesiv, M. *et al.* Global forest management data for 2015 at a 100 m resolution. *Sci Data* **9**, 199 (2022).
25. FAOSTAT. https://www.fao.org/faostat/en/#data.
26. Harris, N. L. *et al.* Global maps of twenty-first century forest carbon fluxes. *Nat. Clim. Chang.* **11**, 234–240 (2021).
27. Poggio, L. *et al.* SoilGrids 2.0: producing soil information for the globe with quantified spatial uncertainty. *SOIL* **7**, 217–240 (2021).
28. Wernet, G. *et al.* The ecoinvent database version 3 (part I): overview and methodology. *Int J Life Cycle Assess* **21**, 1218–1230 (2016).
29. Carlson, K. M. *et al.* Greenhouse gas emissions intensity of global croplands. *Nature Clim Change* **7**, 63–68 (2017).
30. Anderson, C. M., Bicalho, T., Wallace, E., Letts, T. & Stevenson, M. Forest, Land and Agriculture Science-Based Target-Setting Guidance. (2022).
31. WRI & WBCSD. Greenhouse Gas Protocol Land Sector and Removals Guidance.
32. Roebeling, P. C. & Hendrix, E. M. T. Land speculation and interest rate subsidies as a cause of deforestation: The role of cattle ranching in Costa Rica. *Land Use Policy* **27**, 489–496 (2010).
33. Junquera, V. & Grêt-Regamey, A. Crop booms at the forest frontier: Triggers, reinforcing dynamics, and the diffusion of knowledge and norms. *Global Environmental Change* **57**, 101929 (2019).
34. Earthsight. *Grand Theft Chaco: The Luxury Cars Made with Leather from the Stolen Lands of an Uncontacted Tribe*. https://www.earthsight.org.uk/media/download/962 (2020).
35. Barona, E., Ramankutty, N., Hyman, G. & Coomes, O. T. The role of pasture and soybean in deforestation of the Brazilian Amazon. *Environ. Res. Lett.* **5**, 024002 (2010).
36. Graesser, J., Aide, T. M., Grau, H. R. & Ramankutty, N. Cropland/pastureland dynamics and the slowdown of deforestation in Latin America. *Environ. Res. Lett.* **10**, 034017 (2015).
37. Levis, C. *et al.* Help restore Brazil's governance of globally important ecosystem services. *Nature Ecology & Evolution* **4**, 172–173 (2020).
38. Müller, R., Müller, D., Schierhorn, F., Gerold, G. & Pacheco, P. Proximate causes of deforestation in the Bolivian lowlands: an analysis of spatial dynamics. *Reg Environ Change* **12**, 445–459 (2012).
39. Müller, R., Pacheco, P. & Montero, J. C. *The Context of Deforestation and Forest Degradation in Bolivia: Drivers, Agents and Institutions*. (Center for International Forestry Research (CIFOR), Bogor, Indonesia, 2014).
40. Nomura, K. *et al.* Oil palm concessions in southern Myanmar consist mostly of unconverted forest. *Sci Rep* **9**, 11931 (2019).
41. Warren-Thomas, E., Ahrends, A., Wang, Y., Wang, M. M. H. & Jones, J. P. G. Rubber's inclusion in zero-deforestation legislation is necessary but not sufficient to reduce impacts on biodiversity. *Conservation Letters* **16**, e12967 (2023).
42. Blaser-Hart, W. J. *et al.* The effectiveness of cocoa agroforests depends on shade-tree canopy height. *Agriculture, Ecosystems & Environment* **322**, 107676 (2021).
43. Perfecto, I., Jiménez-Soto, M. E. & Vandermeer, J. Coffee Landscapes Shaping the Anthropocene: Forced Simplification on a Complex Agroecological Landscape. *Current Anthropology* **60**, S236–S250 (2019).
44. Ramage, M. H. *et al.* The wood from the trees: The use of timber in construction. *Renewable and Sustainable Energy Reviews* **68**, 333–359 (2017).
45. Meyfroidt, P. Trade-offs between environment and livelihoods: Bridging the global land use and food security discussions. *Global Food Security* **16**, 9–16 (2018).
46. Feng, Y. *et al.* Doubling of annual forest carbon loss over the tropics during the early twenty-first century. *Nat Sustain* **5**, 444–451 (2022).
47. Global Forest Watch (GFW). Global Deforestation Rates & Statistics by Country. https://www.globalforestwatch.org/dashboards/global/.
48. GADM. Database of Global Administrative Areas (Version v4.1). https://gadm.org/.
49. Tyukavina, A. *et al.* Global Trends of Forest Loss Due to Fire From 2001 to 2019. *Frontiers in Remote Sensing* **3**, (2022).
50. Reiner, F. *et al.* More than one quarter of Africa's tree cover is found outside areas previously classified as forest. *Nat Commun* **14**, 2258 (2023).
51. Hansen, M. C., Stehman, S. V. & Potapov, P. V. Quantification of global gross forest cover loss. *Proceedings of the National Academy of Sciences* **107**, 8650–8655 (2010).
52. Margono, B. A., Potapov, P. V., Turubanova, S., Stolle, F. & Hansen, M. C. Primary forest cover loss in Indonesia over 2000–2012. *Nature Clim Change* **4**, 730–735 (2014).
53. Maraseni, T. N., Son, H. L., Cockfield, G., Duy, H. V. & Nghia, T. D. Comparing the financial returns from acacia plantations with different plantation densities and rotation ages in Vietnam. *Forest Policy and Economics* **83**, 80–87 (2017).
54. Steinfeld, H. *Livestock's Long Shadow: Environmental Issues and Options*. (Food and Agriculture Organization of the United Nations, Rome, 2006).
55. Harris, N., Goldman, E. D. & Gibbes, S. *Spatial Database of Planted Trees (SDPT Version 1.0)*. https://www.wri.org/research/spatial-database-planted-trees-sdpt-version-10 (2019).

56. Gibbs, H. K. *et al.* Brazil's Soy Moratorium. *Science* **347**, 377–378 (2015).
57. Gaveau, D. L. A. *et al.* Rapid conversions and avoided deforestation: Examining four decades of industrial plantation expansion in Borneo. *Sci. Rep.* **6**, (2016).
58. Li, W. *et al.* Gross and net land cover changes in the main plant functional types derived from the annual ESA CCI land cover maps (1992–2015). *Earth System Science Data* **10**, 219–234 (2018).
59. Harper, K. L. *et al.* A 29-year time series of annual 300m resolution plant-functional-type maps for climate models. *Earth System Science Data* **15**, 1465–1499 (2023).
60. Opio, C. *et al. Greenhouse Gas Emissions from Ruminant Supply Chains – a Global Life Cycle Assessment*. (Food and Agriculture Organization of the United Nations, Rome, 2013).
61. Instituto Brasileiro de Geografia e Estatística (IBGE). IBGE Produção Agrícola Municipal. https://sidra.ibge.gov.br/pesquisa/pam/tabelas (2022).
62. Persson, U. M., Henders, S. & Cederberg, C. A method for calculating a land-use change carbon footprint (LUC-CFP) for agricultural commodities – applications to Brazilian beef and soy, Indonesian palm oil. *Global Change Biology* **20**, 3482–3491 (2014).
63. Maciel, V. G. *et al.* Towards a non-ambiguous view of the amortization period for quantifying direct land-use change in LCA. *Int J Life Cycle Assess* **27**, 1299–1315 (2022).
64. Mokany, K., Raison, R. J. & Prokushkin, A. S. Critical analysis of root : shoot ratios in terrestrial biomes. *Global Change Biology* **12**, 84–96 (2006).
65. Dinerstein, E. *et al.* An Ecoregion-Based Approach to Protecting Half the Terrestrial Realm. *BioScience* **67**, 534–545 (2017).
66. *2006 IPCC Guidelines for National Greenhouse Gas Inventories - Volume 4*. https://www.ipcc.ch/report/2006-ipcc-guidelines-for-national-greenhouse-gas-inventories/ (2006).
67. Global Forest Watch (GFW). Global Peatlands. https://data.globalforestwatch.org/datasets/gfw::global-peatlands/about.
68. John Couwenberg. *Emission Factors for Managed Peat Soils - An Analysis of IPCC Default Values*. https://www.wetlands.org/publications/emission-factors-for-managed-peat-soils-an-analysis-of-ipcc-default-values/ (2009).
69. Günther, A. *et al.* Prompt rewetting of drained peatlands reduces climate warming despite methane emissions. *Nat Commun* **11**, 1644 (2020).
70. Cooper, H. V. *et al.* Greenhouse gas emissions resulting from conversion of peat swamp forest to oil palm plantation. *Nat Commun* **11**, 407 (2020).

Supplementary Information

Global patterns of commodity-driven deforestation and associated carbon emissions

Chandrakant Singh[1,2] and U. Martin Persson[1]

[1]Department of Space, Earth and Environment, Chalmers University of Technology, Gothenburg, Sweden
[2]Stockholm Resilience Centre, Stockholm University, Stockholm, Sweden

Corresponding authors: Chandrakant Singh (chandrakant.singh@chalmers.se) and
U. Martin Persson (martin.persson@chalmers.se)

Table of Contents

Table of Contents **1**

Supplementary Figures **2**

Supplementary Fig. 1 | Identifying the major drivers of deforestation and associated carbon emissions 2

Supplementary Fig. 2 | Geographical overview of commodity-driven deforestation 3

Supplementary Fig. 3 | Top-50 deforestation-risk country-commodity pairs 4

Supplementary Fig. 4 | Temporal trends of deforestation and carbon emissions for different geographical regions 5

Supplementary Fig. 5 | Framework for distinguishing natural forest loss and loss over managed forests.... 6

Supplementary Fig. 6 | Visual representation of the statistical deforestation attribution (i.e., two-step land balance model) 7

Supplementary Fig. 7 | Agriculture-driven deforestation estimates for Brazil in 2022 are overestimated, due to the lack of more detailed spatial data 8

Supplementary Tables **9**

Supplementary Table 1 | Countries and their respective geographical regions reported in this study 9

Supplementary Table 2 | Commodities and their respective commodity groups reported in this study 12

Supplementary Table 3 | Datasets used in this study and their description 16

Supplementary Table 4 | Scoring individual datasets for attribution and quality assessment 18

Supplementary Table 5 | Pre-processing and attribution assumptions for the spatial datasets 19

Supplementary Table 6 | AGB-to-BGB conversion ratio for different biomes 21

Supplementary Table 7 | Loss of soil organic carbon (SOC) across different land use and biomes 21

Supplementary Table 8 | Plant carbon stocks of replacing commodities and commodity groups across different biomes 22

Supplementary Table 9 | Emission factor used to estimate carbon emissions from deforestation on peatlands 23

Supplementary Table 10 | Criteria's for scoring different aspects of spatial datasets 24

Supplementary Table 11 | The FAO flags, their description and associated penalisation 25

References **26**

Supplementary Figures

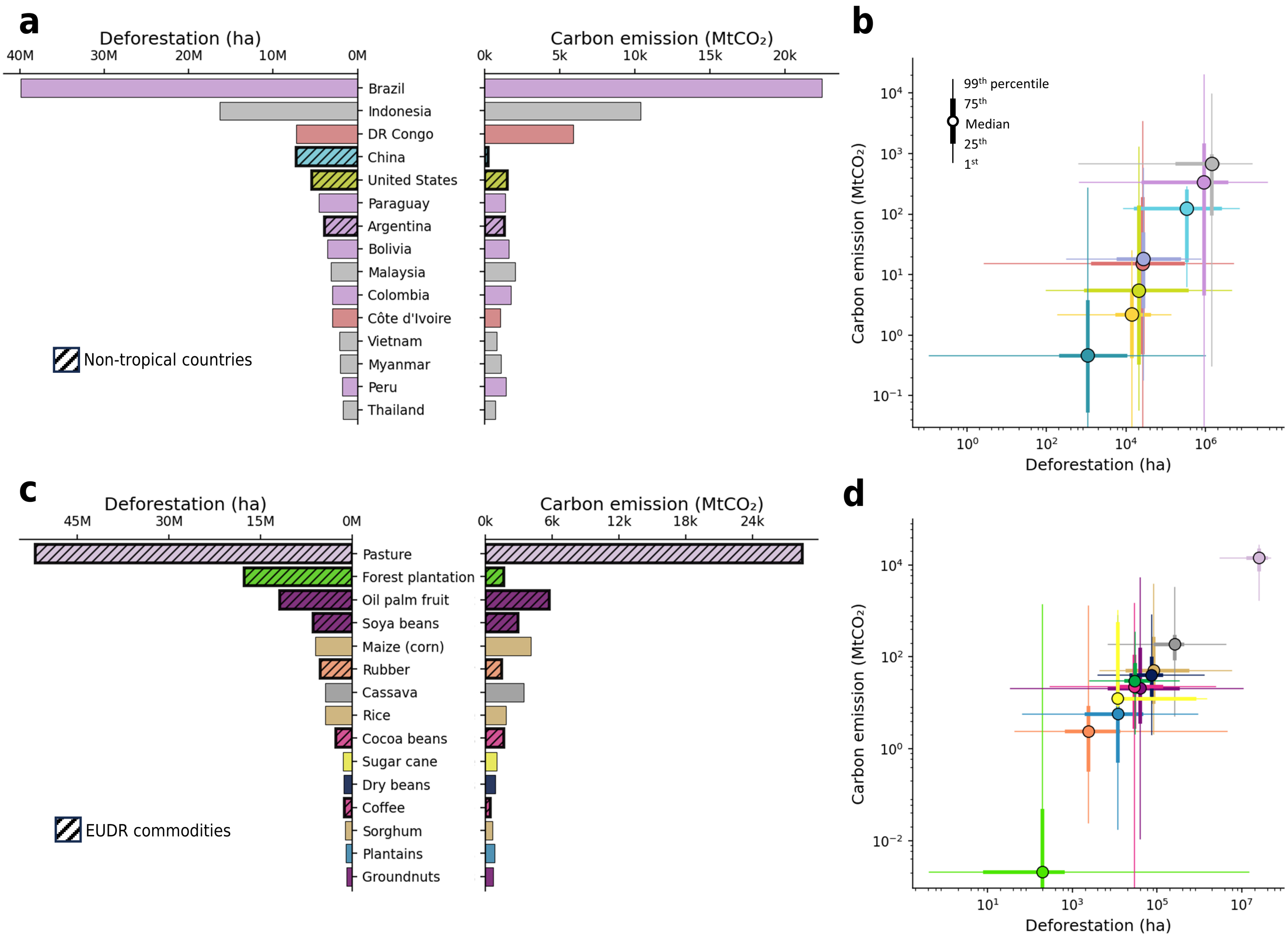

Supplementary Fig. 1 | Identifying the major drivers of deforestation and associated carbon emissions. (a,c) Bar plots feature dominant contributors of deforestation and their associated emissions across different geographical regions and commodity groups. (b,d) Scatter plots delineate the correlation and spread between deforestation area (ha) and carbon emissions (MtCO2). Here, 'pasture' includes both 'cattle meat' and 'leather' production, while 'forest plantations' aggregate deforestation from all forestry commodities. The colour scheme for geographical regions (in a,b) and commodity groups (in b,d) is the same as in Fig. 3.

Supplementary Fig. 2 | Geographical overview of commodity-driven deforestation. Similar to Fig. 3b in the main text, this figure shows agriculture and forestry-driven deforestation and corresponding carbon emissions across but here broken down by different geographical regions. In the concentric rings, the outer ring depicts the proportion of deforestation by area, while the inner ring shows carbon emissions, including peatland emissions, with selected major deforestation commodities accentuated along the periphery of the concentric circles.

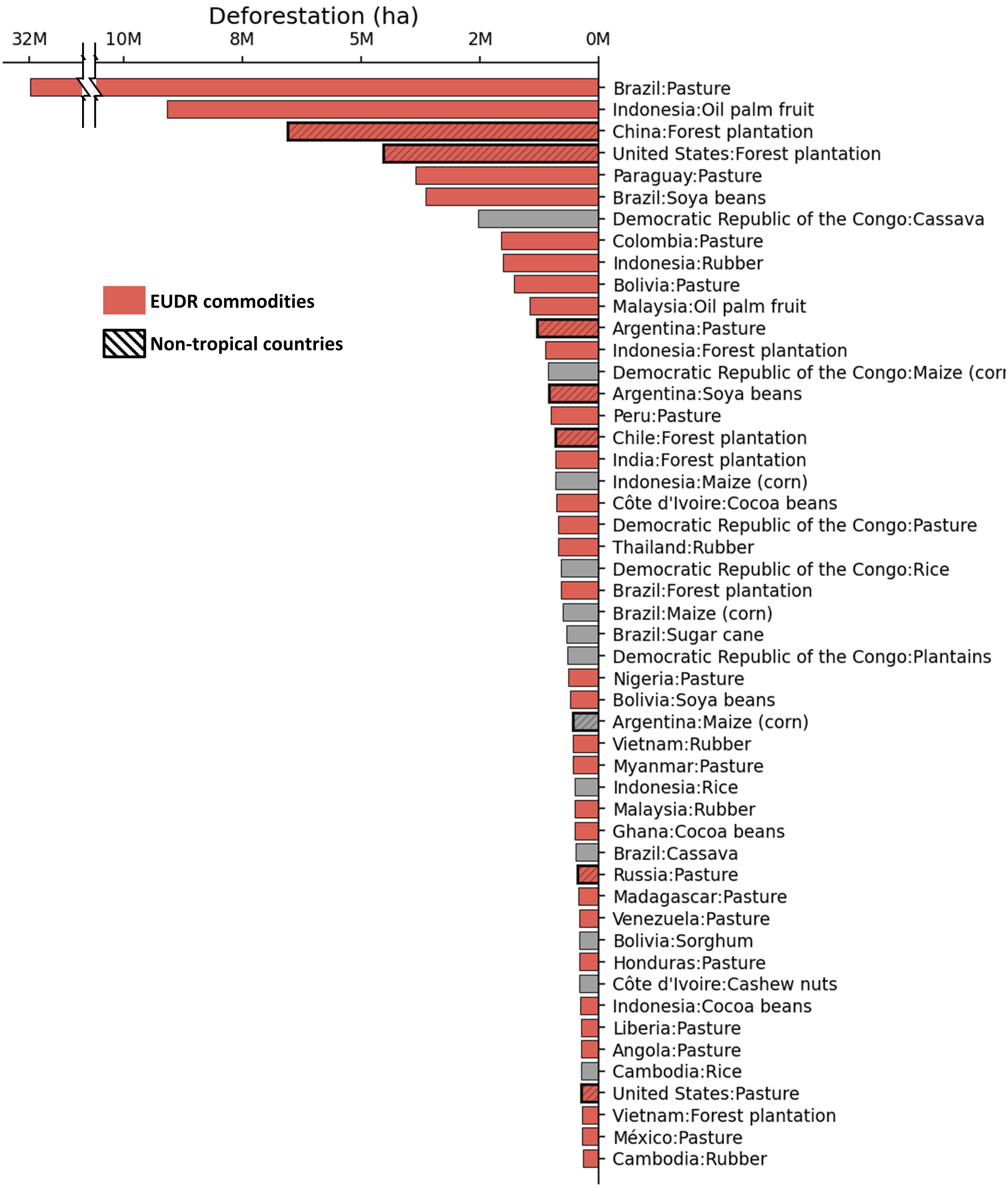

Supplementary Fig. 3 | Top-50 deforestation-risk country-commodity pairs. Bar plots feature dominant contributors to deforestation.

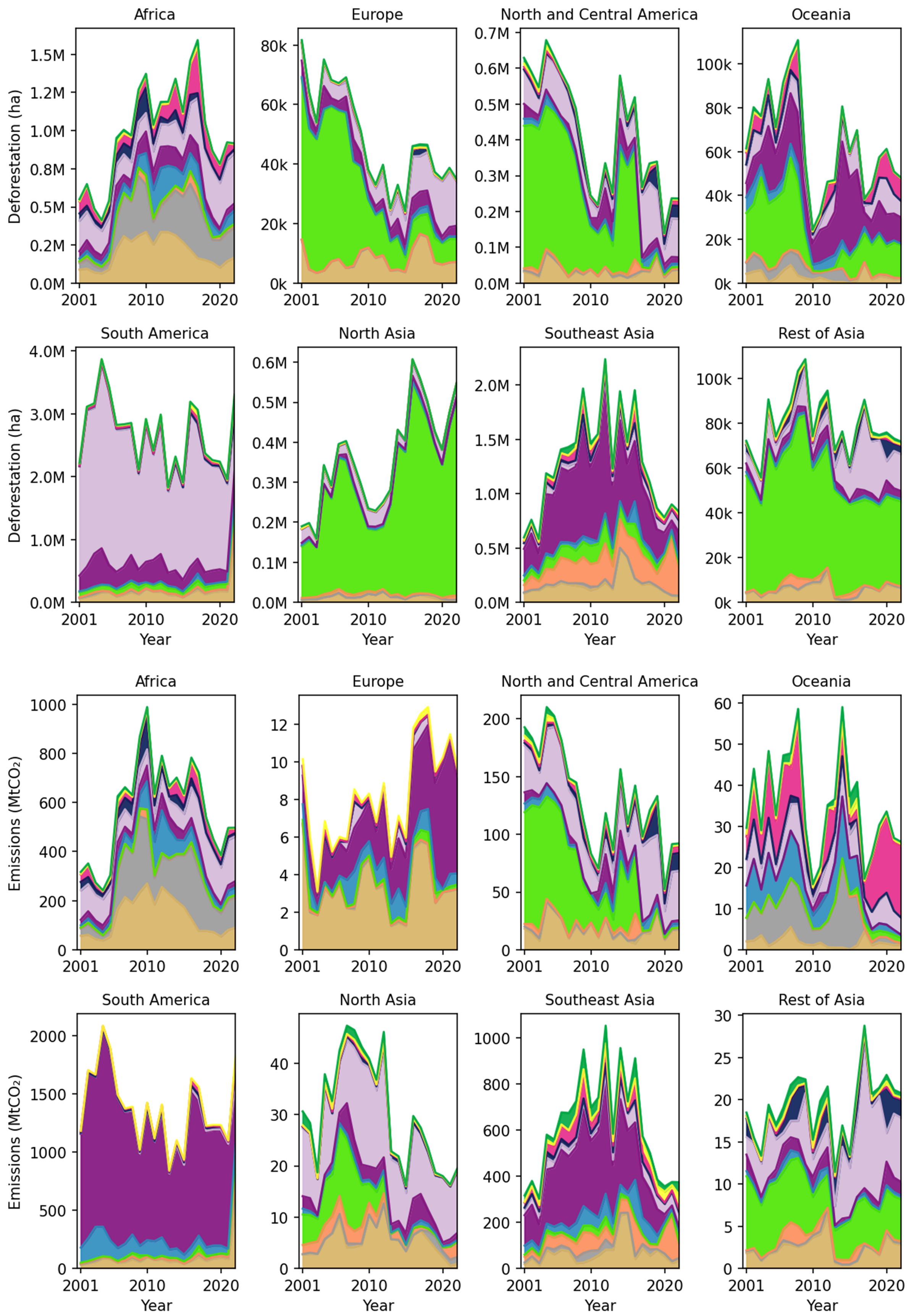

Supplementary Fig. 4 | Temporal trends of deforestation and carbon emissions for different geographical regions. The colour scheme for commodity groups is the same as in Fig. 3b in the main text.

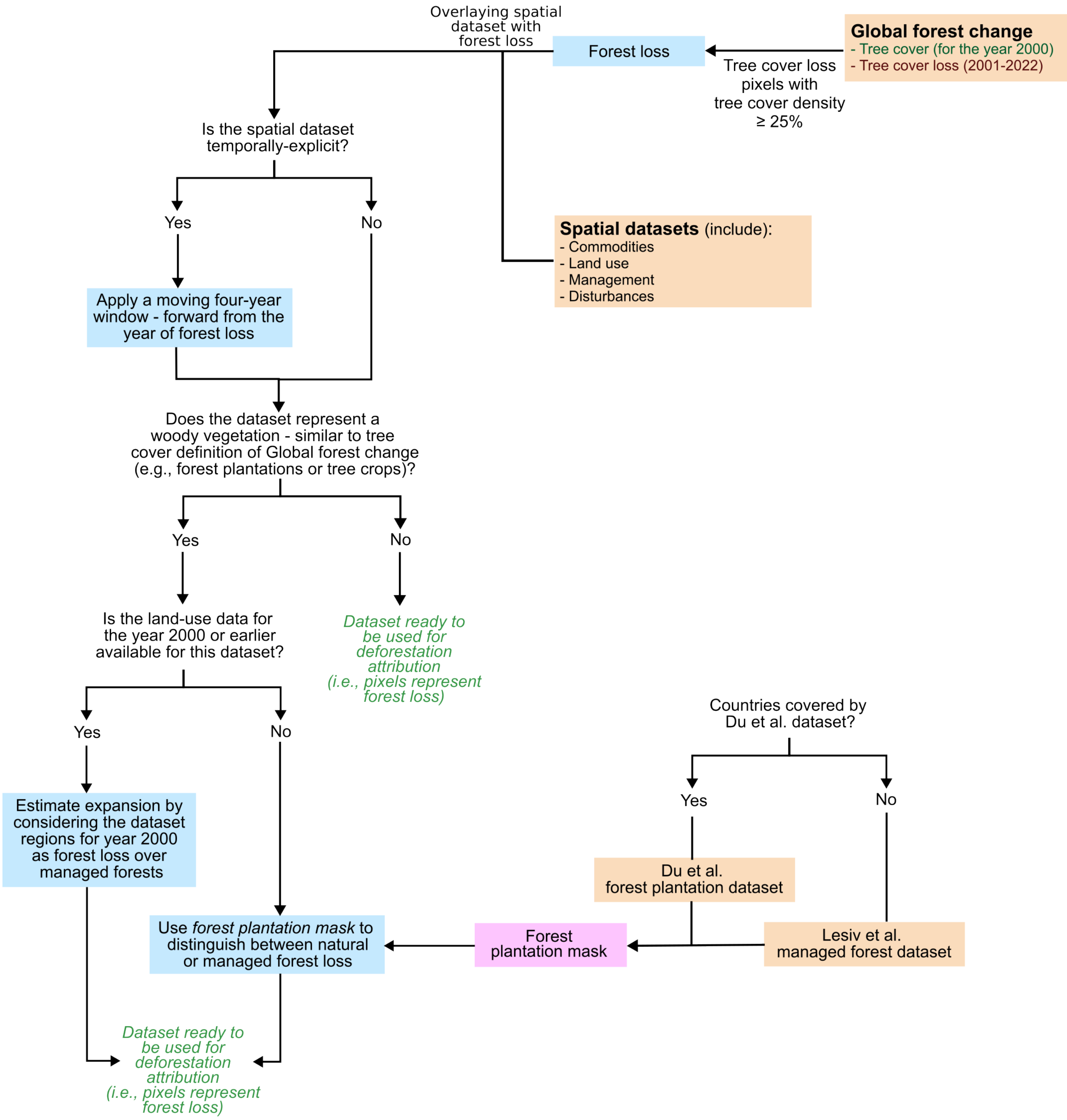

Supplementary Fig. 5 | Framework for distinguishing natural forest loss and loss over managed forests. Global forest plantation mask based on Du et al.[1] and Lesiv et al.[2].

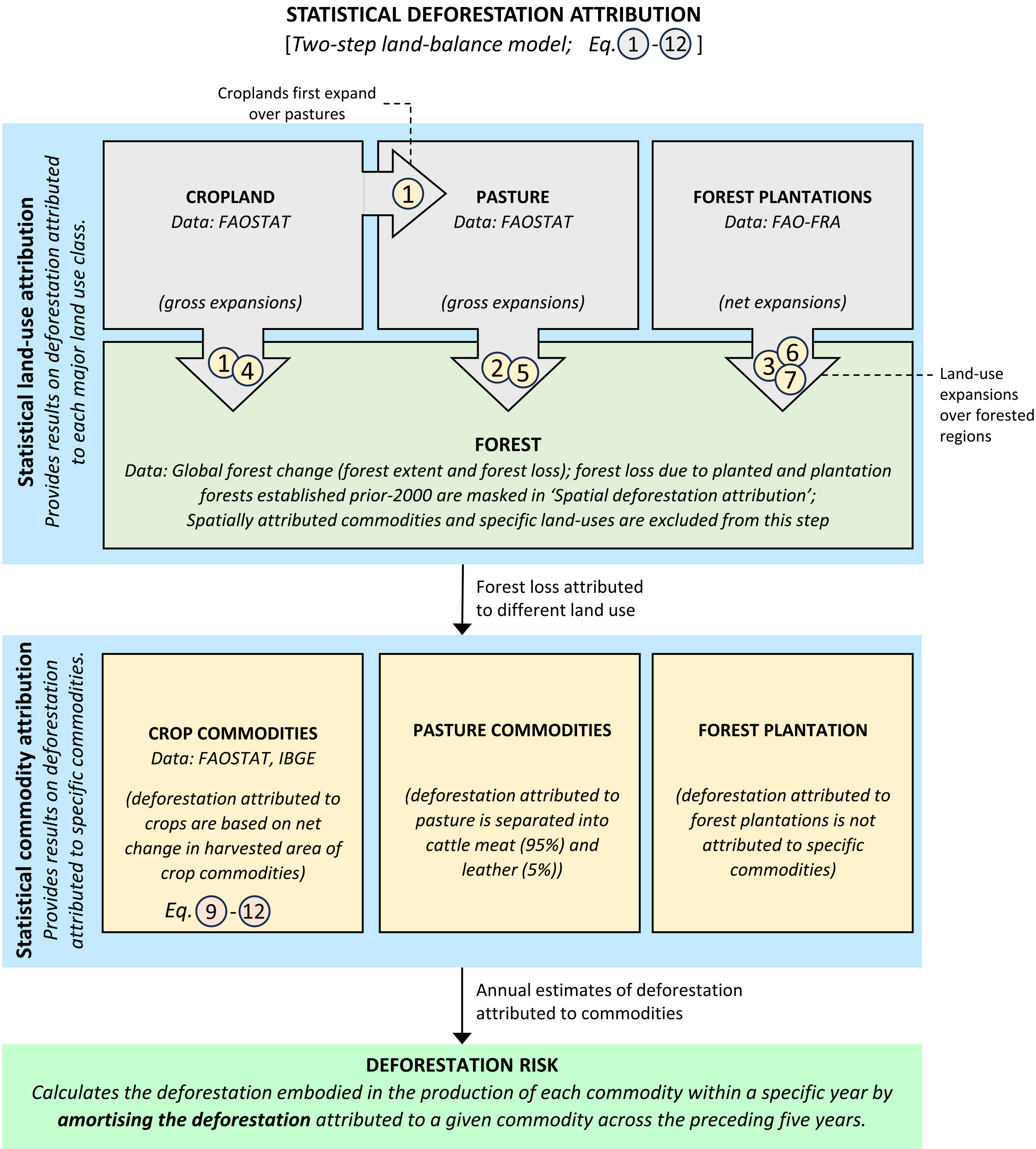

Supplementary Fig. 6 | Visual representation of the statistical deforestation attribution (i.e., two-step land balance model). The figure is adapted from ref.[3].

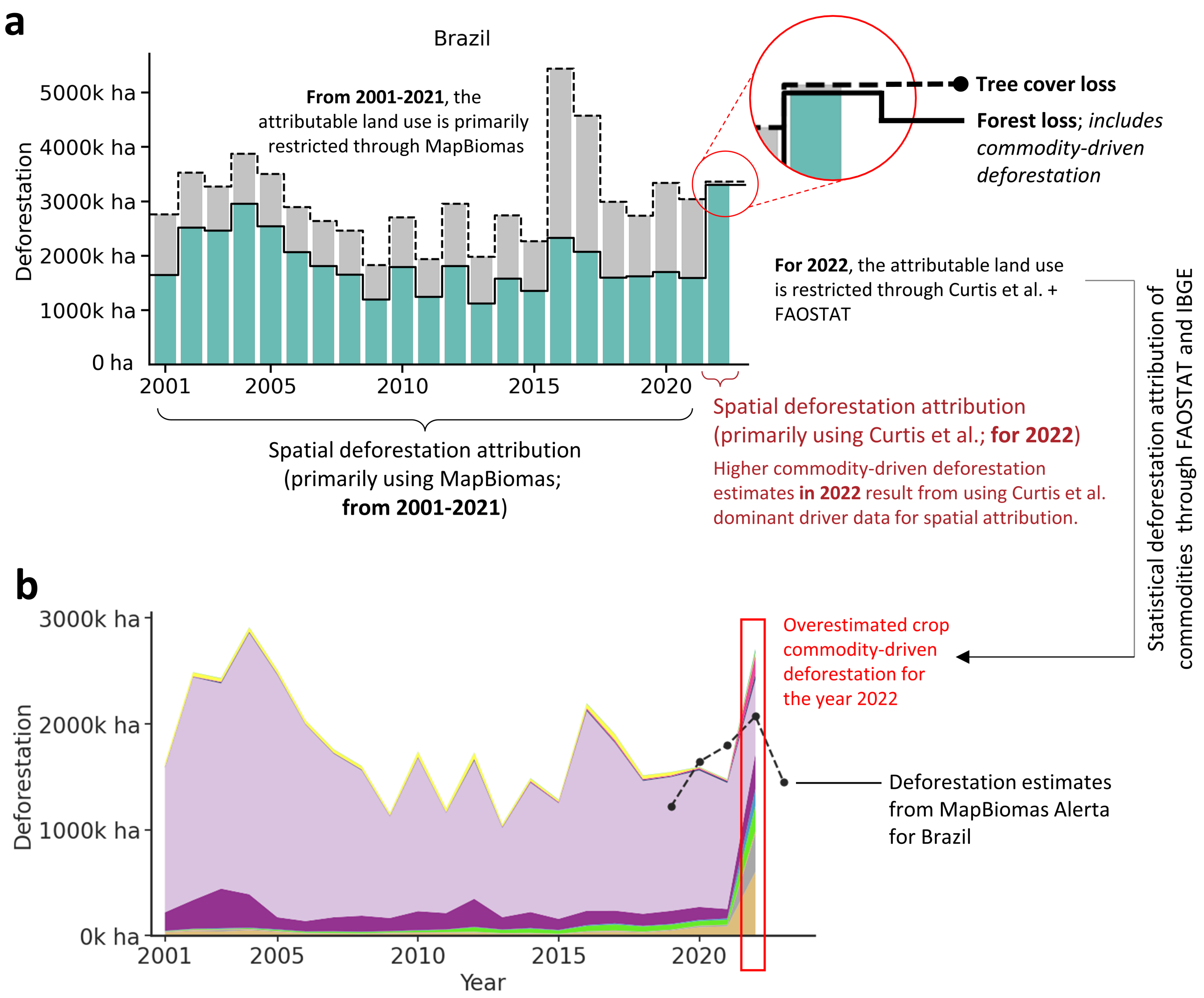

Supplementary Fig. 7 | Agriculture-driven deforestation estimates for Brazil in 2022 are overestimated, due to the lack of more detailed spatial data. (a) The figure shows results after spatial deforestation attribution (as highlighted in Fig. 1). The colour scheme (in a) is the same as Fig. 2. (b) The stack plot shows temporal trends of commodity groups. The colour scheme (in b) is the same as Fig. 3. Curtis et al.[4] refer to the dominant driver of forest loss dataset. MapBiomas Alerta[5] is a system that provides satellite-based alerts for deforestation across Brazil.

Supplementary Tables

Supplementary Table 1 | Countries and their respective geographical regions reported in this study. Note that the table below excludes countries that either experienced no deforestation or lacked FAOSTAT agricultural statistics for the period from 2001 to 2021.

Sr. No.	Producer country	Geographical region
1	Algeria	Africa
2	Angola	Africa
3	Benin	Africa
4	Botswana	Africa
5	Burkina Faso	Africa
6	Burundi	Africa
7	Cabo Verde	Africa
8	Cameroon	Africa
9	Central African Republic	Africa
10	Chad	Africa
11	Comoros	Africa
12	Côte d'Ivoire	Africa
13	Democratic Republic of the Congo	Africa
14	Egypt	Africa
15	Equatorial Guinea	Africa
16	Eritrea	Africa
17	Ethiopia	Africa
18	Gabon	Africa
19	Gambia	Africa
20	Ghana	Africa
21	Guinea	Africa
22	Guinea-Bissau	Africa
23	Kenya	Africa
24	Lesotho	Africa
25	Liberia	Africa
26	Libya	Africa
27	Madagascar	Africa
28	Malawi	Africa
29	Mali	Africa
30	Mauritania	Africa
31	Mauritius	Africa
32	Morocco	Africa
33	Mozambique	Africa
34	Namibia	Africa
35	Niger	Africa
36	Nigeria	Africa
37	Republic of the Congo	Africa
38	Rwanda	Africa
39	Senegal	Africa
40	Seychelles	Africa
41	Sierra Leone	Africa
42	Somalia	Africa
43	South Africa	Africa
44	Sudan (includes both Sudan and South Sudan)	Africa
45	Swaziland	Africa
46	São Tomé and Príncipe	Africa
47	Tanzania	Africa
48	Togo	Africa

49	Tunisia	Africa
50	Uganda	Africa
51	Zambia	Africa
52	Zimbabwe	Africa
53	Albania	Europe
54	Austria	Europe
55	Belarus	Europe
56	Belgium	Europe
57	Bosnia and Herzegovina	Europe
58	Bulgaria	Europe
59	Croatia	Europe
60	Czechia	Europe
61	Denmark	Europe
62	Estonia	Europe
63	Finland	Europe
64	France	Europe
65	Germany	Europe
66	Greece	Europe
67	Hungary	Europe
68	Ireland	Europe
69	Italy	Europe
70	Latvia	Europe
71	Lithuania	Europe
72	Luxembourg	Europe
73	Malta	Europe
74	Moldova	Europe
75	Netherlands	Europe
76	North Macedonia	Europe
77	Norway	Europe
78	Poland	Europe
79	Portugal	Europe
80	Romania	Europe
81	Serbia (includes both Serbia and Montenegro)	Europe
82	Slovakia	Europe
83	Slovenia	Europe
84	Spain	Europe
85	Sweden	Europe
86	Switzerland	Europe
87	Ukraine	Europe
88	United Kingdom	Europe
89	Antigua and Barbuda	North and Central America
90	Bahamas	North and Central America
91	Barbados	North and Central America
92	Belize	North and Central America
93	Canada	North and Central America
94	Costa Rica	North and Central America
95	Cuba	North and Central America
96	Dominica	North and Central America
97	Dominican Republic	North and Central America
98	El Salvador	North and Central America
99	Guatemala	North and Central America
100	Haiti	North and Central America
101	Honduras	North and Central America
102	Jamaica	North and Central America
103	México	North and Central America
104	Nicaragua	North and Central America

105	Panama	North and Central America
106	Puerto Rico	North and Central America
107	Saint Kitts and Nevis	North and Central America
108	Saint Lucia	North and Central America
109	Saint Vincent and the Grenadines	North and Central America
110	United States	North and Central America
111	Australia	Oceania
112	Fiji	Oceania
113	Micronesia	Oceania
114	New Caledonia	Oceania
115	New Zealand	Oceania
116	Papua New Guinea	Oceania
117	Solomon Islands	Oceania
118	Vanuatu	Oceania
119	Argentina	South America
120	Bolivia	South America
121	Brazil	South America
122	Chile	South America
123	Colombia	South America
124	Ecuador	South America
125	Grenada	South America
126	Guyana	South America
127	Paraguay	South America
128	Peru	South America
129	Suriname	South America
130	Trinidad and Tobago	South America
131	Uruguay	South America
132	Venezuela	South America
133	China (includes Hong Kong and Macao, excludes Taiwan)	North Asia
134	Kazakhstan	North Asia
135	Mongolia	North Asia
136	Russia	North Asia
137	Brunei	Southeast Asia
138	Cambodia	Southeast Asia
139	Indonesia	Southeast Asia
140	Laos	Southeast Asia
141	Malaysia	Southeast Asia
142	Myanmar	Southeast Asia
143	Philippines	Southeast Asia
144	Singapore	Southeast Asia
145	Thailand	Southeast Asia
146	Timor-Leste	Southeast Asia
147	Vietnam	Southeast Asia
148	Afghanistan	Rest of Asia
149	Armenia	Rest of Asia
150	Azerbaijan	Rest of Asia
151	Bangladesh	Rest of Asia
152	Bhutan	Rest of Asia
153	Cyprus	Rest of Asia
154	Georgia	Rest of Asia
155	India	Rest of Asia
156	Iran	Rest of Asia
157	Iraq	Rest of Asia
158	Israel	Rest of Asia
159	Japan	Rest of Asia

160	Jordan	Rest of Asia
161	Kyrgyzstan	Rest of Asia
162	Lebanon	Rest of Asia
163	Maldives	Rest of Asia
164	Nepal	Rest of Asia
165	North Korea	Rest of Asia
166	Oman	Rest of Asia
167	Pakistan	Rest of Asia
168	Palestine	Rest of Asia
169	South Korea	Rest of Asia
170	Sri Lanka	Rest of Asia
171	Syria	Rest of Asia
172	Tajikistan	Rest of Asia
173	Turkey	Rest of Asia
174	Turkmenistan	Rest of Asia
175	Uzbekistan	Rest of Asia
176	Yemen	Rest of Asia

Supplementary Table 2 | Commodities and their respective commodity groups reported in this study. Note that while FAOSTAT tracks 171 agricultural commodities, those not contributing to deforestation are omitted from the table below.

Sr. No.	Commodity	Commodity group
1	Barley	Cereals
2	Buckwheat	Cereals
3	Canary seed	Cereals
4	Cereals n.e.c.	Cereals
5	Fonio	Cereals
6	Maize (corn)	Cereals
7	Millet	Cereals
8	Mixed grain	Cereals
9	Oats	Cereals
10	Quinoa	Cereals
11	Rice	Cereals
12	Rye	Cereals
13	Sorghum	Cereals
14	Triticale	Cereals
15	Wheat	Cereals
16	Cassava, fresh	Edible roots and tubers with high starch or inulin content
17	Edible roots and tubers with high starch or inulin content, n.e.c., fresh	Edible roots and tubers with high starch or inulin content
18	Potatoes	Edible roots and tubers with high starch or inulin content
19	Sweet potatoes	Edible roots and tubers with high starch or inulin content
20	Taro	Edible roots and tubers with high starch or inulin content
21	Yams	Edible roots and tubers with high starch or inulin content
22	Yautia	Edible roots and tubers with high starch or inulin

		content
23	Abaca, manila hemp, raw	Fibre crops
24	Agave fibres, raw, n.e.c.	Fibre crops
25	Flax, processed but not spun	Fibre crops
26	Flax, raw or retted	Fibre crops
27	Jute, raw or retted	Fibre crops
28	Kenaf, and other textile bast fibres, raw or retted	Fibre crops
29	Natural rubber in primary forms	Fibre crops
30	Other fibre crops, raw, n.e.c.	Fibre crops
31	Peppermint, spearmint	Fibre crops
32	Pyrethrum, dried flowers	Fibre crops
33	Ramie, raw or retted	Fibre crops
34	Seed cotton, unginned	Fibre crops
35	Sisal, raw	Fibre crops
36	True hemp, raw or retted	Fibre crops
37	Unmanufactured tobacco	Fibre crops
38	All forest plantation commodities	Forest plantation
39	Almonds, in shell	Fruit and nuts
40	Apples	Fruit and nuts
41	Apricots	Fruit and nuts
42	Areca nuts	Fruit and nuts
43	Avocados	Fruit and nuts
44	Bananas	Fruit and nuts
45	Blueberries	Fruit and nuts
46	Cashew nuts, in shell	Fruit and nuts
47	Cashewapple	Fruit and nuts
48	Cherries	Fruit and nuts
49	Chestnuts, in shell	Fruit and nuts
50	Cranberries	Fruit and nuts
51	Currants	Fruit and nuts
52	Dates	Fruit and nuts
53	Figs	Fruit and nuts
54	Gooseberries	Fruit and nuts
55	Grapes	Fruit and nuts
56	Guavas	Fruit and nuts
57	Hazelnuts, in shell	Fruit and nuts
58	Kiwi fruit	Fruit and nuts
59	Kola nuts	Fruit and nuts
60	Lemons and limes	Fruit and nuts
61	Locust beans (carobs)	Fruit and nuts
62	Mangoes	Fruit and nuts
63	Mangoes, guavas and mangosteens	Fruit and nuts
64	Oranges	Fruit and nuts
65	Other berries and fruits of the genus vaccinium n.e.c.	Fruit and nuts
66	Other citrus fruit, n.e.c.	Fruit and nuts
67	Other fruits, n.e.c.	Fruit and nuts
68	Other nuts (excluding wild edible nuts and groundnuts), in shell, n.e.c.	Fruit and nuts
69	Other pome fruits	Fruit and nuts
70	Other stone fruits	Fruit and nuts
71	Other tropical and subtropical fruits, n.e.c.	Fruit and nuts
72	Other tropical fruits, n.e.c.	Fruit and nuts
73	Papayas	Fruit and nuts
74	Peaches and nectarines	Fruit and nuts
75	Pears	Fruit and nuts
76	Persimmons	Fruit and nuts
77	Pineapples	Fruit and nuts

78	Pistachios, in shell	Fruit and nuts
79	Plantains and cooking bananas	Fruit and nuts
80	Plums and sloes	Fruit and nuts
81	Pomelos and grapefruits	Fruit and nuts
82	Quinces	Fruit and nuts
83	Raspberries	Fruit and nuts
84	Sour cherries	Fruit and nuts
85	Strawberries	Fruit and nuts
86	Tangerines and mandarins	Fruit and nuts
87	Tangerines, mandarins, clementines	Fruit and nuts
88	Walnuts, in shell	Fruit and nuts
89	Castor oil seeds	Oilseeds and oleaginous fruits
90	Coconuts, in shell	Oilseeds and oleaginous fruits
91	Groundnuts, excluding shelled	Oilseeds and oleaginous fruits
92	Hempseed	Oilseeds and oleaginous fruits
93	Jojoba seeds	Oilseeds and oleaginous fruits
94	Kapok fruit	Oilseeds and oleaginous fruits
95	Karite nuts (sheanuts)	Oilseeds and oleaginous fruits
96	Linseed	Oilseeds and oleaginous fruits
97	Melonseed	Oilseeds and oleaginous fruits
98	Mustard seed	Oilseeds and oleaginous fruits
99	Oil palm fruit	Oilseeds and oleaginous fruits
100	Olives	Oilseeds and oleaginous fruits
101	Other oil seeds, n.e.c.	Oilseeds and oleaginous fruits
102	Palm nuts and kernels	Oilseeds and oleaginous fruits
103	Poppy seed	Oilseeds and oleaginous fruits
104	Rape or colza seed	Oilseeds and oleaginous fruits
105	Safflower seed	Oilseeds and oleaginous fruits
106	Sesame seed	Oilseeds and oleaginous fruits
107	Soya beans	Oilseeds and oleaginous fruits
108	Sunflower seed	Oilseeds and oleaginous fruits
109	Tallowtree seeds	Oilseeds and oleaginous fruits
110	Tung nuts	Oilseeds and oleaginous fruits
111	Cattle meat	Pasture
112	Leather	Pasture
113	Bambara beans, dry	Pulses (dried leguminous vegetables)
114	Beans, dry	Pulses (dried leguminous vegetables)
115	Broad beans and horse beans, dry	Pulses (dried leguminous vegetables)
116	Chick peas, dry	Pulses (dried leguminous vegetables)
117	Cow peas, dry	Pulses (dried leguminous vegetables)
118	Lentils, dry	Pulses (dried leguminous vegetables)
119	Lupins	Pulses (dried leguminous vegetables)
120	Other pulses n.e.c.	Pulses (dried leguminous vegetables)
121	Peas, dry	Pulses (dried leguminous vegetables)
122	Pigeon peas, dry	Pulses (dried leguminous vegetables)
123	Pulses, n.e.c.	Pulses (dried leguminous vegetables)
124	Vetches	Pulses (dried leguminous vegetables)
125	Anise, badian, coriander, cumin, caraway, fennel and juniper berries, raw	Stimulant, spice and aromatic crops
126	Chicory roots	Stimulant, spice and aromatic crops
127	Chillies and peppers, dry (Capsicum spp., Pimenta spp.), raw	Stimulant, spice and aromatic crops
128	Cinnamon and cinnamon-tree flowers, raw	Stimulant, spice and aromatic crops
129	Cloves (whole stems), raw	Stimulant, spice and aromatic crops
130	Cocoa beans	Stimulant, spice and aromatic crops
131	Coffee, green	Stimulant, spice and aromatic crops
132	Ginger, raw	Stimulant, spice and aromatic crops
133	Hop cones	Stimulant, spice and aromatic crops

134	MatÃ© leaves	Stimulant, spice and aromatic crops
135	Nutmeg, mace, cardamoms, raw	Stimulant, spice and aromatic crops
136	Other stimulant, spice and aromatic crops, n.e.c.	Stimulant, spice and aromatic crops
137	Pepper (Piper spp.), raw	Stimulant, spice and aromatic crops
138	Stimulant, spice and aromatic crops, n.e.c.	Stimulant, spice and aromatic crops
139	Tea leaves	Stimulant, spice and aromatic crops
140	Vanilla, raw	Stimulant, spice and aromatic crops
141	Other sugar crops n.e.c.	Sugar crops
142	Sugar beet	Sugar crops
143	Sugar cane	Sugar crops
144	Artichokes	Vegetables
145	Asparagus	Vegetables
146	Broad beans and horse beans, green	Vegetables
147	Cabbages	Vegetables
148	Cantaloupes and other melons	Vegetables
149	Carrots and turnips	Vegetables
150	Cassava leaves	Vegetables
151	Cauliflowers and broccoli	Vegetables
152	Chillies and peppers, green (Capsicum spp. and Pimenta spp.)	Vegetables
153	Cucumbers and gherkins	Vegetables
154	Eggplants (aubergines)	Vegetables
155	Green corn (maize)	Vegetables
156	Green garlic	Vegetables
157	Leeks and other alliaceous vegetables	Vegetables
158	Lettuce and chicory	Vegetables
159	Okra	Vegetables
160	Onions and shallots, dry (excluding dehydrated)	Vegetables
161	Onions and shallots, green	Vegetables
162	Other beans, green	Vegetables
163	Other vegetables, fresh n.e.c.	Vegetables
164	Peas, green	Vegetables
165	Pumpkins, squash and gourds	Vegetables
166	Spinach	Vegetables
167	String beans	Vegetables
168	Tomatoes	Vegetables
169	Watermelons	Vegetables

Supplementary Table 3 | Datasets used in this study and their description.

Datasets	Spatial extent	Spatial resolution	Temporal resolution	References
Datasets used for spatial deforestation attribution				
Global forest change-v1.10: Tree cover (2000) and tree cover loss (2001-2022)	Global	30 m	2001-2022	6
Global plantation dataset* *(*Based on the spatial database of planted trees[7])*	Argentina, Australia, Brazil, Cambodia, Cameroon, Chile, China, Colombia, Costa Rica, Democratic Republic of the Congo, Ecuador, European countries, Gabon, Ghana, Guatemala, Honduras, India, Indonesia, Côte d'Ivoire, Japan, Kenya, Liberia, Malawi, Malaysia, Mexico, Myanmar, Nepal, New Zealand, Nicaragua, Nigeria, Pakistan, Panama, Papua New Guinea, Peru, Philippines, Rwanda, Solomon Islands, South Africa, South Korea, Sri Lanka, Thailand, Uruguay, United States, Venezuela, Vietnam	30 m	1982-2020	1
MapBiomas Collection	Brazil, Colombia, Venezuela, Suriname, Guyana, French Guiana, Ecuador, Peru, Bolivia, Paraguay, Uruguay, Argentina, Indonesia	30 m	1985-2021 (for South America, the data starts from 1985, but for Indonesia, the data is available from 2000-2019)	8
Croplands	Global	30 m	Aggregated temporally at every 4-year intervals between 2000-2019	9
Sugarcane	Brazil	30 m	Aggregated temporally using data for year 2016-2019	10
Soya beans	South America	30 m	2001-2022	11
Rice	Northeast and Southeast Asia	10 m	Aggregated temporally using the data for year 2017-2019	12
Rapeseed	Argentina, Europe, United States and Canada	10 m	Aggregated temporally using data for year 2017-2019	13
Maize (corn)	China	30 m	2001-2020	14
Cocoa	Côte d'Ivoire and Ghana	10 m	Aggregated temporally using data for year 2018-2021	15
Coconut	Pan-tropical	20 m	2020	16
Oil palm fruit	Indonesia	Vector	2000-2019	17
	Malaysia and Indonesia# (#Indonesia data not used)	100 m	2001-2018	18
	Pan-tropical	10 m	2019	19
Rubber	Southeast Asia and China	10 m	Aggregated temporally using data for year 2020-2022	20
Forest loss due to fire	Global	30 m	2001-2022	21
Forest management	Global	100 m	Aggregated temporally using data for year 2014-2016	2
Dominant drivers of forest loss	Global	10 km	Aggregated temporally using data for year 2001-2022	4
Datasets used for statistical deforestation attribution				
FAOSTAT-Land use	Global	Aggregated at national level	1961-2021	22

FAOSTAT-Production	Global	Aggregated at national level	1961-2021	[22]
Forest Resource Assessment (FAO-FRA)	Global	Aggregated at national level	1990, 2000, 2010, 2015, 2016, 2017, 2018, 2019, 2020	[23]
Brazilian Institute of Geography and Statistics (IBGE)	Brazil	Aggregated at municipality level	1974-2022	[24]
Crop and grass loss	Global	300 m	1992-2020	[25–27]
Datasets used for estimating carbon emissions				
Aboveground biomass$^{\$}$ *($^{\$}$Used to estimate belowground biomass[28], deadwood and litter carbon stocks[29])*	Global	30 m	2000	[29]
Soil organic carbon stocks	Global	250 m	Aggregated temporally using datasets from several years	[30]
Peatland extent$^{\Phi}$ *($^{\Phi}$Globally aggregated peatland extent is based on refs.[31–35])*	Global	30 m		[36]
Ecoregions	Global	Vector		[37]
Precipitation	Global	5 km	1981-2022	[38]
Elevation	Global	90 m		[39]
Other datasets				
Database of Global Administrative Areas-v4.1 (GADM)	Global	Vector		[40]

Supplementary Table 4 | Scoring individual datasets for attribution and quality assessment. The criteria for the scoring methodology are detailed in Supplementary Table 10. Commodities are attributed in descending order of their scores, starting with the highest-scored commodity and proceeding to the lowest.

Dataset	Space	Time	Explicitness	Score	Special remarks
Oil palm fruit (Indonesia)	1.00	1.00	1.00	**1.00**	Reduce the score by 0.05 for every year after 2019
Maize (China)	0.90	1.00	1.00	**0.97**	
Soya beans (South America)	0.80	1.00	1.00	**0.93**	
Sugarcane (Brazil)	0.90	0.70	1.00	**0.87**	
Oil palm fruit (Malaysia)	0.65	0.90	1.00	**0.85**	Reduce the score by 0.05 for every year after 2018
Cocoa (Côte d'Ivoire and Ghana)	0.95	0.60	1.00	**0.85**	
MapBiomas collection (Commodities)	0.80	1.00	0.70	**0.83**	Includes only explicitly defined commodities
Rice (Asia)	0.90	0.60	1.00	**0.83**	
Rapeseed (North America, Canada, Europe and Chile)	0.85	0.60	1.00	**0.82**	
Rubber (Asia)	0.90	0.50	1.00	**0.80**	
Oil palm fruit (Pan-tropical)	0.75	0.40	1.00	**0.72**	
Coconut (Pan-tropical)	0.70	0.40	1.00	**0.70**	
Global plantation dataset	0.65	0.80	0.65	**0.70**	
MapBiomas collection (Land use)	0.80	1.00	0.30	**0.70**	Includes all land-use classifications excluding commodities
Croplands	0.65	0.80	0.50	**0.65**	
Forest loss due to fire	0.65	1.00	0.10	**0.58**	Dataset not used for attribution, but for screening forest loss due to fire
Global forest change (Forest loss)	0.65	0.85	0.10	**0.53**	
Dominant forest loss drivers	0.10	0.85	0.40	**0.45**	
Subnational stats	1.00	1.00	1.00	-	We do not penalise this dataset when flagging (Eq. 19)
FAOSTAT national stats	0.50	1.00	1.00	-	Besides penalising the dataset based on flags (Eq. 15; Supplementary Table 10), we further reduce the FAOSTAT dataset score by '-0.50/3' for both land use and production statistics individually.

Supplementary Table 5 | Pre-processing and attribution assumptions for the spatial datasets.

Datasets	Pre-processing and attribution assumptions
Global forest change	- Forest loss is only considered for pixels with tree cover ≥ 25%
Global plantation dataset	- Only considered as forest plantation-driven deforestation if the start year of the dataset > 2000. 'Start year' defines the year when the first plantation was established based on the temporal extent of remote sensing datasets - Forest loss pixels classified with start year ≤ 2000 are considered under rotational clearing - *Attribution*: For this dataset, deforestation attribution is not temporally restricted
MapBiomas Collection	- Forest loss is attributed to MapBiomas when a commodity-driven land use occurs within a four-year window from the year of forest loss - In case of multiple land use changes occurring within this four-year window, forest plantations will be prioritised over perennial crops, and perennial crops prioritised over pastures, followed by temporary crops - If MapBiomas(t) land use is the same as MapBiomas(2000), we consider forest loss as 'historical/rotational clearing' - *Attribution*: For this dataset, deforestation attribution is temporally restricted to 2021; except for Indonesia, it is temporally restricted to 2019
Croplands	- Forest loss recorded from 2001 to 2003 is attributed to cropland only if cropland extent is defined for the period of 2000-2003 - Forest loss recorded from 2001 to 2007 is attributed to cropland defined for the period of 2004-2007. The delay between forest loss and cropland extent is given to accommodate for forest loss and establishment of cropland - Forest loss recorded from 2005 to 2011 is attributed to cropland defined for the period of 2008-2011 - Forest loss recorded from 2008 to 2015 is attributed to cropland defined for the period of 2012-2015 - Forest loss recorded from 2012 to 2019 is attributed to cropland defined for the period of 2016-2019 - *Attribution*: For this dataset, deforestation attribution (following above) is temporally restricted to 2019
Sugarcane	- *Attribution*: For this dataset, deforestation attribution is temporally restricted to 2019
Soya beans	- Forest loss is attributed to Soya beans when a Soya bean land use occurs within a four-year window from the year of forest loss - *Attribution*: For this dataset, deforestation attribution is temporally restricted to 2022
Rice	- Resolution of the dataset is downscaled to 30 m (same resolution as Global forest change), determined by the majority of pixels within the designated reducer window - *Attribution*: For this dataset, deforestation attribution takes place to 2019
Rapeseed	- Resolution of the dataset is downscaled to 30 m (same resolution as Global forest change), determined by the majority of pixels within the designated reducer window - *Attribution*: For this dataset, deforestation attribution is temporally restricted to 2019
Maize (corn)	- Forest loss is attributed to Maize when a Maize land use occurs within a four-year window from the year of forest loss - *Attribution*: For this dataset, deforestation attribution is temporally restricted to 2020
Cocoa	- Resolution of the dataset is downscaled to 30 m (same resolution as Global forest change), determined by the majority of pixels within the designated reducer window - Pixels of forest loss classified as Cocoa and overlapping with plantation mask are considered under 'rotational clearing' - *Attribution*: For this dataset, deforestation attribution is temporally restricted to 2021
Coconut	- Resolution of the dataset is downscaled to 30 m (same resolution as Global forest change), determined by the majority of pixels within the designated reducer window - Pixels of forest loss classified as Coconut and overlapping with plantation mask are considered under 'rotational clearing' - *Attribution*: For this dataset, deforestation attribution is temporally restricted to 2020
Oil palm fruit (Indonesia)	- Forest loss occurring in the regions (i.e., delineated within a boundary) of Oil palm plantations for the year 2000 are classified as 'rotational clearing', and these pixels are

	excluded from commodity-driven deforestation - *Attribution*: This dataset is not temporally restricted, thus assuming that if a forest loss occurs in a pixel post-2019 (data's temporal extent), we consider it as forest loss due to Oil palm for that year
Oil palm fruit (Malaysia)	- Forest loss is attributed to Oil palm when an Oil palm land use occurs within a four-year window from the year of forest loss - Pixels of forest loss classified as Oil palm and overlapping with plantation mask are considered under 'rotational clearing' - *Attribution*: This dataset is not temporally restricted, thus assuming that if a forest loss occurs in a pixel post-2018 (data's temporal extent), we consider it as forest loss due to Oil palm for that year
Oil palm fruit (Global)	- Resolution of the dataset is downscaled to 30 m (same resolution as Global forest change), determined by the majority of pixels within the designated reducer window - Pixels of forest loss classified as Oil palm and overlapping with plantation mask are considered under 'rotational clearing' - *Attribution*: For this dataset, deforestation attribution is temporally restricted to 2019
Rubber	- Resolution of the dataset is downscaled to 30 m (same resolution as Global forest change), determined by the majority of pixels within the designated reducer window - Pixels of forest loss classified as Rubber and overlapping with plantation mask are considered under 'rotational clearing' - *Attribution*: For this dataset, deforestation attribution is temporally restricted to 2022
Forest loss due to fire	- Forest loss pixels classified under '1. Forest loss due to other (non-fire) drivers' are open for attribution by other datasets - Forest loss pixels classified under '2. Low certainty of forest loss due to fire' are open for attribution by other datasets - Forest loss pixels classified under '3. Medium' and '4. High' certainty are excluded from commodity-driven deforestation - Forest loss pixels classified under '5. Forest loss due to fire in Africa' are excluded from commodity-driven deforestation
Forest management	- Forest loss is considered 'rotational clearing' if the pixel falls under '20. Naturally regenerating forest with signs of management, e.g., logging, clear cuts etc', '31: Planted forests (rotation >15 years)', '32: Plantation forests (rotation ≤15 years)', '40: Oil palm plantations' and '53: Agroforestry' - The above only applies to the spatial extent of countries covered in Supplementary Table 3 for 'Forest management'
Dominant drivers of forest loss	- Forest loss pixels classified under 'Commodity-driven deforestation' and 'Shifting agriculture' are considered under agricultural-driven deforestation - Forest loss pixels classified under 'Forestry' are considered under forestry-induced deforestation - Forest loss pixels classified under 'Wildfire' and 'Urbanisation' are excluded from commodity-driven deforestation - Pixels of forest loss classified by this dataset and overlapping with plantation mask are considered under 'rotational clearing'

Supplementary Table 6 | AGB-to-BGB conversion ratio for different biomes. These ratios are adapted from ref.[28].

Ecoregion group	Ecoregion	Lower AGB (Mg ha^{-1})	Upper AGB (Mg ha^{-1})	BGB/AGB Ratio
Tropical	Tropical & Subtropical Moist Broadleaf Forests	-	-	0.456
Tropical	Tropical & Subtropical Dry Broadleaf Forests	0	20	0.563
Tropical	Tropical & Subtropical Dry Broadleaf Forests	20	-	0.275
Tropical	Tropical & Subtropical Coniferous Forests	-	-	0.322
Tropical	Tropical & Subtropical Grasslands, Savannas & Shrublands	-	-	1.887
Tropical	Flooded Grasslands & Savannas	-	-	1.098
Tropical	Mediterranean Forests, Woodlands & Scrub	-	-	0.322
Tropical	Deserts & Xeric Shrublands	-	-	1.063
Tropical	Mangroves	-	-	1.098
Temperate	Temperate Broadleaf & Mixed Forests	0	75	0.456
Temperate	Temperate Broadleaf & Mixed Forests	75	150	0.226
Temperate	Temperate Broadleaf & Mixed Forests	150	-	0.241
Temperate	Temperate Conifer Forests	0	50	0.403
Temperate	Temperate Conifer Forests	50	150	0.292
Temperate	Temperate Conifer Forests	150	-	0.201
Temperate	Temperate Grasslands, Savannas & Shrublands	-	-	4.224
Temperate	Montane Grasslands & Shrublands	-	-	1.887
Boreal	Boreal Forests/Taiga	0	75	0.392
Boreal	Boreal Forests/Taiga	75	-	0.239
Boreal	Tundra	-	-	4.804

Supplementary Table 7 | Loss of soil organic carbon (SOC) across different land use and biomes. The values represent the % loss of actual SOC. Note that for depths 30-100 cm, the data is scarce. Thus, we use the 0-100 cm data to estimate SOC loss for 30-100 cm depth. We do this by assuming that SOC $loss_{0\text{-}100\ cm}$ = SOC $loss_{0\text{-}30\ cm}$ + SOC $loss_{30\text{-}100\ cm}$.

		Land use replacing forest (values in %)			
Depth	Ecoregion group	Cropland	Pasture	Plantation	References
0-30 cm	Global	26.6	18	13	[41,42]
0-30 cm	Tropical	29	4	22	[43–45]
0-30 cm	Temperate	31.4	4.15	15	[42,46,47]
0-30 cm	Boreal	21	18†	13†	[48]
30-100 cm	Global	13.8$^{\#}$	9.7$^{\#}$	23$^{\#}$	[41,49]
30-100 cm	Tropical	15	2	7	[45]
30-100 cm	Temperate	25	6.925*	19*	[46]
30-100 cm	Boreal	17.4*	13.85*	18*	

†Imputed using global average estimates

$^{\#}$Values available for depths of 0-100 cm

*Calculated using the average of global and respective ecoregions 0-30m estimates; consider these values for 0-100 cm

Supplementary Table 8 | Plant carbon stocks of replacing commodities and commodity groups across different biomes.

<table>
<tr><th></th><th colspan="3">(Values in MgC ha^{-1})</th><th></th></tr>
<tr><th>Crop or Commodity group</th><th>Tropical</th><th>Temperate</th><th>Boreal</th><th>References</th></tr>
<tr><td>Cereals</td><td>4.44</td><td colspan="2">3.15</td><td>50,51</td></tr>
<tr><td>Maize (corn)</td><td colspan="3">6.3</td><td>50</td></tr>
<tr><td>Rice</td><td colspan="3">4.5</td><td>50</td></tr>
<tr><td>Wheat</td><td colspan="3">2.3</td><td>50</td></tr>
<tr><td>Barley</td><td colspan="3">5.5</td><td>52</td></tr>
<tr><td>Sorghum</td><td colspan="3">4.12</td><td>50</td></tr>
<tr><td>Millet</td><td colspan="3">3.13</td><td>53</td></tr>
<tr><td>Edible roots and tubers with high starch or inulin content</td><td colspan="3">3</td><td>51</td></tr>
<tr><td>Cassava</td><td colspan="3">4.5</td><td>54</td></tr>
<tr><td>Potatoes</td><td colspan="3">0.5</td><td>55</td></tr>
<tr><td>Fibre crops</td><td colspan="3">3.71</td><td>50</td></tr>
<tr><td>Natural rubber in primary forms</td><td colspan="3">79.05</td><td>56</td></tr>
<tr><td>Jute, raw or retted</td><td colspan="3">3.9</td><td>50</td></tr>
<tr><td>Seed cotton, unginned</td><td colspan="3">4.3</td><td>50</td></tr>
<tr><td>Forest plantation</td><td>120.23</td><td>130.99</td><td>96.07</td><td>57</td></tr>
<tr><td>Fruit and nuts</td><td>31.96</td><td colspan="2">39.53</td><td>58,59</td></tr>
<tr><td>Apples</td><td colspan="3">26.48</td><td>60</td></tr>
<tr><td>Bananas</td><td colspan="3">6.2</td><td>61</td></tr>
<tr><td>Cashew nuts, in shell</td><td colspan="3">37.6</td><td>62</td></tr>
<tr><td>Grapes</td><td colspan="3">12.3</td><td>63</td></tr>
<tr><td>Mangoes</td><td colspan="3">84.75</td><td>64</td></tr>
<tr><td>Oranges</td><td colspan="3">7.69</td><td>65</td></tr>
<tr><td>Other citrus fruit, n.e.c.</td><td>20.65</td><td colspan="2">23.73</td><td>61</td></tr>
<tr><td>Plantains and cooking bananas</td><td colspan="3">6.2</td><td>61</td></tr>
<tr><td>Oilseeds and oleaginous fruits</td><td>31.96</td><td colspan="2">39.53</td><td>58,59</td></tr>
<tr><td>Oil palm fruit</td><td colspan="3">52.28</td><td>56</td></tr>
<tr><td>Soya beans</td><td colspan="3">3</td><td>50</td></tr>
<tr><td>Sunflower seed</td><td colspan="3">1.1</td><td>50</td></tr>
<tr><td>Groundnuts, excluding shelled</td><td colspan="3">1.1</td><td>50</td></tr>
<tr><td>Olives</td><td colspan="3">5.3</td><td>66</td></tr>
<tr><td>Coconuts, in shell</td><td>57.38</td><td colspan="2">65.93</td><td>61</td></tr>
<tr><td>Pasture</td><td colspan="3">6.8</td><td>50</td></tr>
<tr><td>Pulses (dried leguminous vegetables)</td><td colspan="3">1.56</td><td>50</td></tr>
<tr><td>Beans, dry</td><td colspan="3">2.39</td><td>53</td></tr>
<tr><td>Chick peas, dry</td><td colspan="3">1.28</td><td>53</td></tr>
<tr><td>Cow peas, dry</td><td colspan="3">1.82</td><td>53</td></tr>
<tr><td>Pigeon peas, dry</td><td colspan="3">3</td><td>53</td></tr>
<tr><td>Lentils, dry</td><td colspan="3">1.25</td><td>53</td></tr>
<tr><td>Peas, dry</td><td colspan="3">0.9</td><td>50</td></tr>
<tr><td>Stimulant, spice and aromatic crops</td><td>31.96</td><td colspan="2">39.53</td><td>58,59</td></tr>
<tr><td>Coffee, green</td><td colspan="3">77.12</td><td>67</td></tr>
<tr><td>Cocoa beans</td><td colspan="3">34.55</td><td>68</td></tr>
<tr><td>Tea leaves</td><td colspan="3">21.06</td><td>69</td></tr>
<tr><td>Sugar crops</td><td colspan="3">10.17</td><td>Average of commodities in the group</td></tr>
<tr><td>Sugar beet</td><td colspan="3">8.32</td><td>55</td></tr>
<tr><td>Sugar cane</td><td colspan="3">12.02</td><td>70</td></tr>
<tr><td>Vegetables</td><td colspan="3">0.43</td><td>71</td></tr>
<tr><td>Cabbages</td><td colspan="3">1.65</td><td>50</td></tr>
<tr><td>Lettuce and chicory</td><td colspan="3">1.15</td><td>72</td></tr>
</table>

Tomatoes	3.48	72
Cauliflowers and broccoli	4.05	72

Supplementary Table 9 | Emission factor used to estimate carbon emissions from deforestation on peatlands.

	(values in $MgCO_2$ ha^{-1} yr^{-1})			
Land use replacing forest	**Tropical**	**Temperate**	**Boreal**	**References**
Cropland	45	28.6	27.9	73
Pasture	37.4	17.95	20.2	74
Plantation	40.34	2.5	6.42	75
Oil palm fruit	54.41			76

Supplementary Table 10 | Criteria's for scoring different aspects of spatial datasets.

Aspect	Criteria	Penalisation
Space (representing both resolution and area of focus)	Perfect score is given when the pixel size is ≤ 10m and is explicitly mapped for a country	0
	Resolution of 20 m	-0.05
	Resolution of 30 m	-0.1
	Resolution of 100 m	-0.3
	Resolution of 1 km	-0.5
	Resolution of 10 km	-0.75
	Mapped for two countries	-0.05
	Mapped for more than two countries or a continent	-0.1
	Multiple continents	-0.15
	Mapped globally	-0.25
Time (representing temporal resolution and standalone ability of the data to differentiate pre- and post-2000's deforestation)	Perfect score is given when the dataset is available from 2001-2022 for herbaceous crops, and at least the year 2000- or prior-onwards for woody vegetation crops (i.e., tree crops) and forest plantations (allowing for differentiation between post-2000's deforestation from the rotational clearing of managed plantations)	0
	For tree crops and forest plantations, deforestation is not differentiable from rotational clearing (need to be complimented with plantation mask to extract this information)	Using Du et al: -0.1 Using Lesiv et al: -0.2
	After the latest detection year (in cases allowed)	-0.05 each year
	Temporally-aggregated detection based on a single year of remote sensing dataset	-0.3
	Temporally-aggregated detection based on 2-3 years of remote sensing dataset	-0.2
	Temporally-aggregated detection based on 4-6 years of remote sensing dataset	-0.1
	Temporally-aggregated detection based on >6 years of remote sensing dataset	0
	Temporally-explicit detection every 2-3 years between 2001-2022	-0.1
	Temporally-explicit detection every 4-6 years between 2001-2022	-0.2
	Starting year of detection is 1-5 years away from 2001 (i.e., the first year of analysed deforestation)	-0.05
	Starting year of detection is 6-10 years away from 2001	-0.1
	Starting year of detection is 11-15 years away from 2001	-0.15
	Starting year of detection is >15 years away from 2001	-0.2
Explicitness (representation of the deforestation driver and consideration given to training algorithm of the data)	Perfect score is given to datasets that maps a single commodity, where model training is performed using field samples	0
	When training is primarily based on remote sensing trends, without using field samples (including visual interpretations)	-0.5
	When multiple commodities or land uses are predicted by the same model using the same field samples	-0.1
	Dataset maps two or more than two commodities (differentiable)	-0.2
	Dataset maps a single land use	-0.3
	Dataset maps two or more than two different land uses (differentiable)	-0.4
	Dataset maps two or more than two different land uses (indifferentiable, i.e., mosaics)	-0.6
	Information about forest loss drivers is unavailable	-0.9

Supplementary Table 11 | The FAO flags, their description and associated penalisation. A detailed description of FAO flags is documented in ref.[77].

Flag	Description	Penalisation
A	**Official figure**: Value provided as official when the source agency assigns sufficient confidence that it is not expected to be dramatically revised	0
B	**Time series break**: Observations are characterised as such when different content exists or a different methodology has been applied to this observation as compared with the preceding one	-0.10
E	**Estimated value**: Observation obtained through an estimation methodology or based on the use of a limited amount of data	-0.20
I	**Imputed value**: Observation imputed by a receiving agency to replace or fill gaps in reported data series	-0.30
P	**Provisional value**: An observation is characterised as "provisional" when the source agency – while it bases its calculations on its standard production methodology – considers that the data, almost certainly, are expected to be revised	-0.40
T	**Unofficial figure**: Observations are "temporary" or "tentative", indicating that the figure should be used with caution and may be subject to revision or replacement with official statistics once they become available.	-0.40
X	**Figure from international organisations**: Observation from an international or a supranational organisation that does not use any flagging system in data sharing	-0.50
M	**Missing value**: Used to denote empty cells resulting from the impossibility to collect a statistical value	-0.70
Z	**Authors gap filling**: Gap filled by authors of this study (*not part of FAO flags*)	-0.70

References

1. Du, Z. *et al.* A global map of planting years of plantations. *Sci Data* **9**, 141 (2022).
2. Lesiv, M. *et al.* Global forest management data for 2015 at a 100 m resolution. *Sci Data* **9**, 199 (2022).
3. Pendrill, F., Persson, U. M., Godar, J. & Kastner, T. Deforestation displaced: trade in forest-risk commodities and the prospects for a global forest transition. *Environ. Res. Lett.* **14**, 055003 (2019).
4. Curtis, P. G., Slay, C. M., Harris, N. L., Tyukavina, A. & Hansen, M. C. Classifying drivers of global forest loss. *Science* **361**, 1108–1111 (2018).
5. MapBiomas Alerta. https://alerta.mapbiomas.org/en.
6. Hansen, M. C. *et al.* High-Resolution Global Maps of 21st-Century Forest Cover Change. *Science* **342**, 850–853 (2013).
7. Harris, N., Goldman, E. D. & Gibbes, S. *Spatial Database of Planted Trees (SDPT Version 1.0)*. https://www.wri.org/research/spatial-database-planted-trees-sdpt-version-10 (2019).
8. MapBiomas. *MapBiomas General "Handbook": Algorithm Theoretical Basis Document (ATBD)*. https://mapbiomas-br-site.s3.amazonaws.com/ATBD_Collection_7_v2.pdf (2022).
9. Potapov, P. *et al.* Global maps of cropland extent and change show accelerated cropland expansion in the twenty-first century. *Nat Food* **3**, 19–28 (2022).
10. Zheng, Y., dos Santos Luciano, A. C., Dong, J. & Yuan, W. High-resolution map of sugarcane cultivation in Brazil using a phenology-based method. *Earth System Science Data* **14**, 2065–2080 (2022).
11. Song, X.-P. *et al.* Massive soybean expansion in South America since 2000 and implications for conservation. *Nat Sustain* 1–9 (2021) doi:10.1038/s41893-021-00729-z.
12. Han, J. *et al.* NESEA-Rice10: high-resolution annual paddy rice maps for Northeast and Southeast Asia from 2017 to 2019. *Earth System Science Data* **13**, 5969–5986 (2021).
13. Han, J. *et al.* The RapeseedMap10 database: annual maps of rapeseed at a spatial resolution of 10m based on multi-source data. *Earth System Science Data* **13**, 2857–2874 (2021).
14. Peng, Q. *et al.* A twenty-year dataset of high-resolution maize distribution in China. *Sci Data* **10**, 658 (2023).
15. Kalischek, N. *et al.* Cocoa plantations are associated with deforestation in Côte d'Ivoire and Ghana. *Nat Food* **4**, 384–393 (2023).
16. Descals, A. *et al.* High-resolution global map of closed-canopy coconut palm. *Earth System Science Data* **15**, 3991–4010 (2023).
17. Gaveau, D. L. A. *et al.* Slowing deforestation in Indonesia follows declining oil palm expansion and lower oil prices. *PLOS ONE* **17**, e0266178 (2022).
18. Xu, Y. *et al.* Annual oil palm plantation maps in Malaysia and Indonesia from 2001 to 2016. *Earth System Science Data* **12**, 847–867 (2020).
19. Descals, A. *et al.* High-resolution global map of smallholder and industrial closed-canopy oil palm plantations. *Earth System Science Data* **13**, 1211–1231 (2021).
20. Wang, Y. *et al.* High-resolution maps show that rubber causes substantial deforestation. *Nature* **623**, 340–346 (2023).
21. Tyukavina, A. *et al.* Global Trends of Forest Loss Due to Fire From 2001 to 2019. *Frontiers in Remote Sensing* **3**, (2022).
22. FAOSTAT. https://www.fao.org/faostat/en/#data.
23. FAO-FRA. Global Forest Resource Assessment 2020. https://fra-data.fao.org/assessments/fra/2020 (2023).
24. Instituto Brasileiro de Geografia e Estatística (IBGE). IBGE Produção Agrícola Municipal. https://sidra.ibge.gov.br/pesquisa/pam/tabelas (2022).
25. Li, W. *et al.* Gross and net land cover changes in the main plant functional types derived from the annual ESA CCI land cover maps (1992–2015). *Earth System Science Data* **10**, 219–234 (2018).
26. Harper, K. L. *et al.* A 29-year time series of annual 300m resolution plant-functional-type maps for climate models. *Earth System Science Data* **15**, 1465–1499 (2023).
27. Copernicus Climate Change Service. Land cover classification gridded maps from 1992 to present derived from satellite observations. ECMWF https://doi.org/10.24381/CDS.006F2C9A (2019).
28. Mokany, K., Raison, R. J. & Prokushkin, A. S. Critical analysis of root : shoot ratios in terrestrial biomes. *Global Change Biology* **12**, 84–96 (2006).
29. Harris, N. L. *et al.* Global maps of twenty-first century forest carbon fluxes. *Nat. Clim. Chang.* **11**, 234–240 (2021).
30. Poggio, L. *et al.* SoilGrids 2.0: producing soil information for the globe with quantified spatial uncertainty. *SOIL* **7**, 217–240 (2021).
31. Crezee, B. *et al.* Mapping peat thickness and carbon stocks of the central Congo Basin using field data. *Nat. Geosci.* **15**, 639–644 (2022).
32. Gumbricht, T. *et al.* An expert system model for mapping tropical wetlands and peatlands reveals South America as the largest contributor. *Global Change Biology* **23**, 3581–3599 (2017).
33. Hastie, A. *et al.* Risks to carbon storage from land-use change revealed by peat thickness maps of Peru. *Nat. Geosci.* **15**, 369–374 (2022).
34. Xu, J., Morris, P. J., Liu, J. & Holden, J. PEATMAP: Refining estimates of global peatland distribution based on a meta-analysis. *CATENA* **160**, 134–140 (2018).
35. Miettinen, J., Shi, C. & Liew, S. C. Land cover distribution in the peatlands of Peninsular Malaysia, Sumatra and Borneo in 2015 with changes since 1990. *Global Ecology and Conservation* **6**, 67–78 (2016).
36. Global Forest Watch (GFW). Global Peatlands. https://data.globalforestwatch.org/datasets/gfw::global-peatlands/about.
37. Dinerstein, E. *et al.* An Ecoregion-Based Approach to Protecting Half the Terrestrial Realm. *BioScience* **67**, 534–545 (2017).

38. Funk, C. *et al.* The climate hazards infrared precipitation with stations—a new environmental record for monitoring extremes. *Scientific Data* **2**, 150066 (2015).
39. Jarvis, A., Guevara, E., Reuter, H. I. & Nelson, A. D. Hole-filled SRTM for the globe : version 4 : data grid. (2008).
40. GADM. Database of Global Administrative Areas (Version v4.1). https://gadm.org/.
41. Sanderman, J., Hengl, T. & Fiske, G. J. Soil carbon debt of 12,000 years of human land use. *Proceedings of the National Academy of Sciences* **114**, 9575–9580 (2017).
42. Guo, L. B. & Gifford, R. M. Soil carbon stocks and land use change: a meta analysis. *Global Change Biology* **8**, 345–360 (2002).
43. Don, A., Schumacher, J. & Freibauer, A. Impact of tropical land-use change on soil organic carbon stocks – a meta-analysis. *Global Change Biology* **17**, 1658–1670 (2011).
44. Powers, J. S., Corre, M. D., Twine, T. E. & Veldkamp, E. Geographic bias of field observations of soil carbon stocks with tropical land-use changes precludes spatial extrapolation. *Proceedings of the National Academy of Sciences* **108**, 6318–6322 (2011).
45. Veldkamp, E., Schmidt, M., Powers, J. S. & Corre, M. D. Deforestation and reforestation impacts on soils in the tropics. *Nat Rev Earth Environ* **1**, 590–605 (2020).
46. Poeplau, C. *et al.* Temporal dynamics of soil organic carbon after land-use change in the temperate zone – carbon response functions as a model approach. *Global Change Biology* **17**, 2415–2427 (2011).
47. Dlamini, P., Chivenge, P. & Chaplot, V. Overgrazing decreases soil organic carbon stocks the most under dry climates and low soil pH: A meta-analysis shows. *Agriculture, Ecosystems & Environment* **221**, 258–269 (2016).
48. Wei, X., Shao, M., Gale, W. & Li, L. Global pattern of soil carbon losses due to the conversion of forests to agricultural land. *Sci Rep* **4**, 4062 (2014).
49. Beillouin, D. *et al.* A global meta-analysis of soil organic carbon in the Anthropocene. *Nat Commun* **14**, 3700 (2023).
50. Mathew, I., Shimelis, H., Mutema, M. & Chaplot, V. What crop type for atmospheric carbon sequestration: Results from a global data analysis. *Agriculture, Ecosystems & Environment* **243**, 34–46 (2017).
51. Wiesmeier, M. *et al.* Estimation of past and recent carbon input by crops into agricultural soils of southeast Germany. *European Journal of Agronomy* **61**, 10–23 (2014).
52. Durán Zuazo, V. H., Francia Martínez, J. R., Pleguezuelo, C. R. R. & Tavira, S. C. Biomass carbon stock in relation to different land uses in a semiarid environment. *Journal of Land Use Science* **9**, 474–486 (2014).
53. Kuyah, S. *et al.* Grain legumes and dryland cereals contribute to carbon sequestration in the drylands of Africa and South Asia. *Agriculture, Ecosystems & Environment* **355**, 108583 (2023).
54. K, R. & B, B. Potential of wastelands for carbon sequestration- A review. *Int. J. Chem. Stud.* **8**, 2873–2881 (2020).
55. Koga, N. *et al.* Estimating net primary production and annual plant carbon inputs, and modelling future changes in soil carbon stocks in arable farmlands of northern Japan. *Agriculture, Ecosystems & Environment* **144**, 51–60 (2011).
56. Guillaume, T. *et al.* Carbon costs and benefits of Indonesian rainforest conversion to plantations. *Nat Commun* **9**, 2388 (2018).
57. Bukoski, J. J. *et al.* Rates and drivers of aboveground carbon accumulation in global monoculture plantation forests. *Nat Commun* **13**, 4206 (2022).
58. Brakas, S. G. & Aune, J. B. Biomass and Carbon Accumulation in Land Use Systems of Claveria, the Philippines. in *Carbon Sequestration Potential of Agroforestry Systems: Opportunities and Challenges* (eds. Kumar, B. M. & Nair, P. K. R.) 163–175 (Springer Netherlands, Dordrecht, 2011). doi:10.1007/978-94-007-1630-8_9.
59. Schafer, L. J., Lysák, M. & Henriksen, C. B. Tree layer carbon stock quantification in a temperate food forest: A peri-urban polyculture case study. *Urban Forestry & Urban Greening* **45**, 126466 (2019).
60. Zahoor, S. *et al.* Apple-based agroforestry systems for biomass production and carbon sequestration: implication for food security and climate change contemplates in temperate region of Northern Himalaya, India. *Agroforest Syst* **95**, 367–382 (2021).
61. Toensmeier, E. & Herren, H. *The Carbon Farming Solution: A Global Toolkit of Perennial Crops and Regenerative Agriculture Practices for Climate Change Mitigation and Food Security*. (Chelsea Green Publishing, White River Junction, Vermont, UNITED STATES, 2016).
62. Victor, A. D., Valery, N. N., Boris, N., Aimé, V. B. T. & Louis, Z. Carbon storage in cashew plantations in Central Africa: case of Cameroon. *Carbon Management* **12**, 25–35 (2021).
63. Morandé, J. A. *et al.* From berries to blocks: carbon stock quantification of a California vineyard. *Carbon Balance and Management* **12**, 5 (2017).
64. Sharma, S., Rana, V. S., Prasad, H., Lakra, J. & Sharma, U. Appraisal of Carbon Capture, Storage, and Utilization Through Fruit Crops. *Frontiers in Environmental Science* **9**, (2021).
65. Sahoo, U. K., Nath, A. J. & Lalnunpuii, K. Biomass estimation models, biomass storage and ecosystem carbon stock in sweet orange orchards: Implications for land use management. *Acta Ecologica Sinica* **41**, 57–63 (2021).
66. Lopez-Bellido, P. J., Lopez-Bellido, L., Fernandez-Garcia, P., Muñoz-Romero, V. & Lopez-Bellido, F. J. Assessment of carbon sequestration and the carbon footprint in olive groves in Southern Spain. *Carbon Management* **7**, 161–170 (2016).
67. Singh, K. P. *et al.* Biomass, carbon stock, CO2 mitigation and carbon credits of coffee-based multitier cropping model in Central India. *Environ Monit Assess* **195**, 1250 (2023).
68. Asigbaase, M., Dawoe, E., Lomax, B. H. & Sjogersten, S. Biomass and carbon stocks of organic and conventional cocoa agroforests, Ghana. *Agriculture, Ecosystems & Environment* **306**, 107192 (2021).
69. Das, M. *et al.* Biomass models for estimating carbon storage in *Areca* palm plantations. *Environmental and Sustainability Indicators* **10**, 100115 (2021).
70. Liang, X. *et al.* Quantifying shoot and root biomass production and soil carbon under perennial bioenergy grasses in a subtropical environment. *Biomass and Bioenergy* **128**, 105323 (2019).

71. Toensmeier, E., Ferguson, R. & Mehra, M. Perennial vegetables: A neglected resource for biodiversity, carbon sequestration, and nutrition. *PLOS ONE* **15**, e0234611 (2020).
72. Farina, R. *et al.* Potential carbon sequestration in a Mediterranean organic vegetable cropping system. A model approach for evaluating the effects of compost and Agro-ecological Service Crops (ASCs). *Agricultural Systems* **162**, 239–248 (2018).
73. John Couwenberg. *Emission Factors for Managed Peat Soils - An Analysis of IPCC Default Values*. https://www.wetlands.org/publications/emission-factors-for-managed-peat-soils-an-analysis-of-ipcc-default-values/ (2009).
74. Günther, A. *et al.* Prompt rewetting of drained peatlands reduces climate warming despite methane emissions. *Nat Commun* **11**, 1644 (2020).
75. John Couwenberg. Greenhouse gas emissions from managed peat soils: is the IPCC reporting guidance realistic? *Mires and Peat 8* **Art. 2**, (2011).
76. Cooper, H. V. *et al.* Greenhouse gas emissions resulting from conversion of peat swamp forest to oil palm plantation. *Nat Commun* **11**, 407 (2020).
77. FAO. *Statistical Standard Series: Observation Status Code List (Version 3)*. https://www.fao.org/3/cc6208en/cc6208en.pdf (2023).